

5-11-2013

Sperm Proteins and Chromatin Dynamics associated with Male Fertility

Sule Dogan

Follow this and additional works at: <https://scholarsjunction.msstate.edu/td>

Recommended Citation

Dogan, Sule, "Sperm Proteins and Chromatin Dynamics associated with Male Fertility" (2013). *Theses and Dissertations*. 4031.

<https://scholarsjunction.msstate.edu/td/4031>

This Dissertation - Open Access is brought to you for free and open access by the Theses and Dissertations at Scholars Junction. It has been accepted for inclusion in Theses and Dissertations by an authorized administrator of Scholars Junction. For more information, please contact scholcomm@msstate.libanswers.com.

Sperm proteins and chromatin dynamics associated with male fertility

By

Sule Dogan

A Dissertation
Submitted to the Faculty of
Mississippi State University
in Partial Fulfillment of the Requirements
for the Degree of Doctor of Philosophy
in Life Sciences/Genetics
in the Department of Animal and Dairy Sciences

Mississippi State, Mississippi

May 2013

Copyright by

Sule Dogan

2013

Sperm proteins and chromatin dynamics associated with male fertility

By

Sule Dogan

Approved:

Erdogan Memili
Associate Professor and Graduate
Coordinator of Animal and Dairy Sciences
(Major Professor)

Donna M. Gordon
Assistant Professor of Biological
Sciences
(Committee member)

Jamie Larson
Assistant Professor of Animal and Dairy
Sciences
(Committee member)

David A. Ray
Assistant Professor of Biochemistry,
Molecular Biology, Entomology, and
Plant Pathology
(Committee member)

George M. Hopper
Dean of College of Agriculture
and Life Sciences

Name: Sule Dogan

Date of Degree: May 10, 2013

Institution: Mississippi State University

Major Field: Life Sciences/Genetics

Major Professor: Erdogan Memili

Title of Study: Sperm proteins and chromatin dynamics associated with male fertility

Pages in Study: 96

Candidate for Degree of Doctor of Philosophy

The impacts of the paternal genome and proteins transferred to the oocyte through spermatozoa cannot be neglected during mammalian embryonic development. Studies over the past 40 years suggest that sperm chromatin alterations (such as DNA fragmentation induced by either chromatin condensation errors, apoptosis and/or oxidative stress) might be negatively associated with fertilization and early embryonic development [1, 2], [3] [4]. However, precise molecular mechanisms by which sperm chromatin integrity and sperm proteins impact early embryonic development still remain unclear. Therefore, the objectives of this study were 1) determine DNA fragmentation induced by apoptosis its relationship with male fertility in spermatozoa from bulls with varying fertility, and 2) identify expression dynamics of Protamine 1 and examine chromatin structure in spermatozoa from bulls with varying fertility. To accomplish our goals we determined 1) the DNA damage, phosphatidylserine (PS) translocation, and expression of pro- and anti-apoptotic proteins (BAX and BCL-2) as well as 2) the expression and localization of Protamine 1 (PRM1) with chromatin condensation and protamination in sperm from bulls with varying fertility.

Our results demonstrated that the most relevant fertility markers might be the percentage of necrotic spermatozoa detected by flow cytometry and live spermatozoa determined via eosin-nigrosin staining and that there was no relationship between apoptosis and male fertility. While BCL-2 was not expressed, BAX was identified in bovine spermatozoa. However, the expression of BAX did not differ among groups. In addition, defective chromatin condensation and protamination errors were significantly increased in sperm from low fertility bulls, while the expression of PRM1 was significantly abundant in high fertility bulls. Bull fertility was negatively correlated with protamination errors and defective chromatin condensation, and it was positively correlated with the expression of PRM1.

We concluded that defective sperm DNA condensation, not abortive apoptosis, might be the major reason of male infertility in bulls and that sperm chromatin stability differs among bulls with varying fertility. Improper chromatin packaging during spermatogenesis might be caused by the limited expression and/or mislocalization of PRM1. Thus, inadequate chromatin dynamics were associated with bull infertility, which might lead improper fertilization.

DEDICATION

This study is dedicated to my father, Ibrahim Dogan.

ACKNOWLEDGEMENTS

First of all, I would like to thank my parents Ibrahim Dogan and Vicdan Dogan; sister, Merve Dogan for all of their prayers, encouragements, unconditional love and unlimited support throughout my journey.

I wish to say thank you to my graduate coordinator and also my major advisor, Dr. Erdogan Memili, for all of his guidance, mentoring, support and patience, all of which meant a lot to me. I would like to extend special appreciation to my committee members, Drs. Donna Gordon, Jamie Larson and David Ray for providing me with their guidance in my research project. To my colleagues in the laboratory Kamilah Grant, Melissa Mason, Aruna Govindaraju, Lauren Besler and Rodrigo Vasconcelos, I would simply like to say thank you for all of your encouraging conversations, friendship and unwavering support during my time here.

I also would like to thank my friends on campus, Dr. Huseyin Tunc, Burcu Ellidort-Tunc, Gokce Palak, and Adetokunbo Adedoyin for their support and being such a second family to me here. I could not have done it without you.

Last but not least, I would like to sincerely thank all faculty members, staff and graduate students of the Department of Animal and Dairy Sciences at Mississippi State University for the support during my graduate studies.

TABLE OF CONTENTS

DEDICATION	ii
ACKNOWLEDGEMENTS	iii
LIST OF TABLES	vii
LIST OF FIGURES	viii
CHAPTER	
I. INTRODUCTION	1
Literature Review.....	1
Early embryonic development	2
Spermatogenesis	3
DNA damage in sperm.....	6
Sperm chromatin condensation.....	7
Apoptosis	10
Oxidative stress.....	11
Detection of DNA damage in sperm.....	12
Justification of the study	14
II. INTERRELATIONSHIPS BETWEEN APOPTOSIS AND FERTILITY IN BULL SPERM.....	16
Abstract	16
Introduction.....	17
Material and Methods	19
Determination of bull fertility	19
Isolation of spermatozoa	20
TUNEL Assay.....	21
Annexin V assay	22
Isolation of sperm proteins.....	23
Immunodetection of apoptotic proteins	23
Statistical analysis	24
Results.....	25
Fertility differences among the bulls	26
Extent of DNA damage in sperm.....	26
Detection of apoptosis via annexin V	27

	Detection of apoptotic proteins via immunoblotting	28
	Discussion	29
	Acknowledgements.....	33
III.	DYNAMICS OF SPERM CHROMATIN ASSOCIATED WITH FERTILITY	42
	Abstract	42
	Introduction.....	43
	Material and Methods	45
	Determination of bull fertility	45
	Isolation of spermatozoa	46
	Chromatin maturity and integrity approaches.....	46
	Toluidine blue (TB) cytometry	46
	Sperm Chromatin Dispersion Test (SCD)/Halomax.....	47
	Expression of the PRM1 Approaches	47
	Sperm nuclear protein isolation	47
	Immunodetection of nuclear proteins using WB	49
	Immunocytochemistry and flow cytometry	50
	Flow cytometry	50
	Immunocytochemistry (ICC) and Cell Imaging	51
	Statistical analysis.....	52
	Results.....	53
	Distinct fertility differences exist among the bulls	53
	Extent of proper protamination differs in sperm from high vs. low fertility bulls.....	53
	Fragmentation status of sperm chromatin is different in high vs. low fertility bulls.....	54
	Expression of PRM1 by immunoblotting is diverse in sperm from high vs. low fertility bulls	54
	Flow cytometric analysis of PRM1 expression in sperm from high and low fertility bulls.....	55
	Localization of PRM1 is varying in sperm from high and low fertility bulls.....	56
	Discussion	56
	Acknowledgements.....	60
IV.	CONCLUSIONS.....	69
	DNA damage-induced by apoptosis may not be an indicator for male infertility	69
	Proper condensation of chromatin in sperm is important for sperm function	70

REFERENCES	73
------------------	----

APPENDIX

A. SUPPLEMENTARY PROTOCOLS	83
Fibroblast Cell Culture Protocol	84
Primary Fibroblast Culture	84
Cryopreservation of fibroblast cells	90
Sperm Isolation Protocol	91
The Percoll Stock Solution Protocol	91
Sperm Isolation/ Separation	95

LIST OF TABLES

2.1	Fertility Differences among the bulls.....	34
2.2	Comparison of two groups (high vs. low fertility).....	34
2.3	Pearson correlation coefficients with p-values.....	35
3.1	List of bulls and fertility data used for this study.....	60
3.2	Mean difference of parameters in high vs. low fertility bulls.	61
3.3	Pearson Correlation Coefficients.....	62
A.1	Table A 90% Percoll Recipe	94

LIST OF FIGURES

1.1	Stages of Early Embryonic Development (redesigned based on [8])	3
1.2	DNA Packing in Spermatozoa (revised from [18, 19]).....	9
2.1	Apoptosis signaling pathway	36
2.2	Experimental design	37
2.3	Sperm cell population by flow cytometry	38
2.4	DNA Fragmentation detected by TUNEL assay using fluorescence microscopy	38
2.5	Sperm apoptotic cell population of two bulls with varying fertility by flow cytometry	39
2.6	Eosin/nigrosin staining	39
2.7	BAX, BCL-2 and Beta-Tubulin proteins	40
2.8	The distribution graph of Western Blotting data	41
2.9	Western Blotting negative controls.	41
3.1	Toluidine Blue (TB) Staining Results	62
3.2	HaloMax® (Sperm Chromatin Dispersion) Test Results.....	63
3.3	Protein quantification using micro BCA protein assay	63
3.4	Distribution of chromatin integrity in sperm.....	64
3.5	Coomassie Blue staining of the Acidic-Acid-Urea (AAU) gel.....	64
3.6	Band Intensities of Coomassie Blue staining	65
3.7	Immunoblotting of PRM1	65
3.8	Flow Cytometric histograms	66

3.9	Flow Cytometric Plots	67
3.10	Immunocytochemistry Results	68

CHAPTER I

INTRODUCTION

Literature Review

Following fertilization of matured oocytes by sperm, the development of mammalian embryos initiates as a zygote and continues development to a blastocyst prior to implantation or attachment. Fertility is the capability of natural production of offspring; thereby any damages to gametes in gametogenesis and early embryonic development may cause irreversible, severe alterations in reproduction called infertility. The incidence of infertility in American couples is 15% and male factor fertility makes up 25% of these infertile couples [5]. Moreover, male fertility is considered to be the fertilizing ability of sperm to activate the oocyte and to support early embryonic development. Male infertility is also an essential factor limiting efficient production in the cattle industry. The genetic basis of male infertility can be classified into three forms: pre-testicular, testicular and post-testicular. One of the major reasons of male infertility is sperm dysfunction, which can only be improved by assisted reproductive technologies (ART) [6]. Likewise, male infertility is also categorized as compensatory (sperm viability and motility), and non-compensatory (molecular defects in the sperm) traits in animals [7]. Providing increased numbers of spermatozoa may overcome compensatory fertility problems, but not non-compensatory fertility in animals; which is still a pitfall in the cattle industry.

Early embryonic development

Following ejaculation of sperm, mature spermatozoa travel in the female reproductive tract toward the ampulla of the fallopian tube where spermatozoon fuses into the oocyte; a process known as fertilization. The spermatozoa bypass the obstacles of the female reproductive tract such as low pH, immune cells, cervical villi, mucus secretions, and contractions. To gain the capability to fertilize the egg, spermatozoa must undergo capacitation; a formation process that is a result of a boost in calcium level of a cell. Following capacitation, transformation of lipid production in the cell surface of spermatozoa occurs, leading to hyperactivation where the motility of spermatozoa progressively increases. After spermatozoa reach the oocyte, they still need to pass the cumulus cells surrounding the oocyte. Spermatozoa then pass the zona pellucida (ZP) consisting of a block of ZP proteins by taking advantage of the acrosome reaction where the acrosome enzymes are released. Once spermatozoon penetrates the ZP and enters into the ooplasm, oocyte activation (zona reaction) takes place during which the cortical granules block the zona to polyspermy. By the time spermatozoon enters into the oocyte, cell cycle and meiosis are completed, which leads to the formation of a non-functional second polar body. The fusion of paternal and maternal genomes takes place as pronuclei (PNs) forming a syngamy approximately 24 hours post-fertilization, producing a one cell embryo; the zygote. Following a set of symmetrical cell divisions via mitosis, the zygote enters a cleavage stage producing compact morula and blastocysts consisting of blastomeres about 32-cells and more than 100-cells, respectively. At the last stage of early embryonic development, blastocysts may either invasively or non-invasively

complete the implantation process where they attach to the endometrial surface of the uterus in mammals (See Figure 1.1 for the details) [[6];reviewed by [8, 9]].

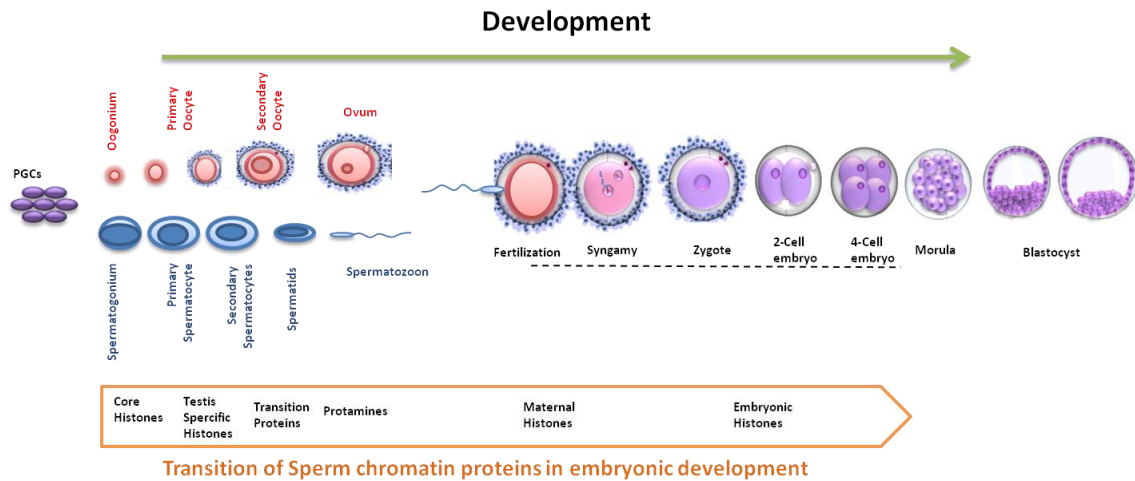


Figure 1.1 Stages of Early Embryonic Development (redesigned based on [8])

Spermatogenesis

As haploid germ cells (n), spermatozoa are consistently generated in seminiferous tubules of the testis via meiosis. In contrast to meiosis, DNA duplication and chromosome segregation sustain over and over again to balance the chromosome numbers in the cell via mitosis, generating a diploid cell ($2n$). Spermatogenesis is a complete process of sperm production via both meiosis and mitosis in mammalian testis, containing three cellular phases: proliferation, meiosis and differentiation. Morphological and nuclear changes take place during spermatogenesis. Subsequently, transcription is halted at certain stages and spermatozoa are thought to be transcriptionally and translationally silent except for mitochondrial DNA activities. At the genomic level, core histones are first replaced by their testis variants and then by transition proteins.

Afterwards, protamines replace the transition proteins and are responsible for the condensation of sperm chromatin. During spermatogenesis, spermatogonia (stem cells) undergo divisions in the testes to form spermatocytes and spermatids; which occur in proliferation and meiosis phases, respectively. Spermatozoa arise from spermatids via spermiogenesis and are then maintained in the epididymis before they are ejaculated in the testicular fluid. Therefore, seminal fluid (semen) contains both spermatozoa and the secretion of accessory sex glands; vesicular glands, prostate gland, and bulbourethral glands, including testicular fluid. Seminal plasma produced by the sex glands is an energy source for spermatozoa during their journey in both the male and female reproductive tracts [6].

Differentiation of male germ cells initiates prenatally. Primitive male germ cells, primordial germ cells (PGC), are originated from epiblastic cells during embryonic development and are then re-located to the extra embryonic mesoderm. Following migration of PGC to the left and right primitive gonads or urogenital ridges during gestation (day 30-64 in bovine, day 7-14 in murine), they keep proliferating. Subsequently, PGCs are localized in the seminiferous tubules of the primitive testes, which are named gonocytes or prespermatogonia, but their mitotic divisions are arrested until birth. The migration of the prespermatogonia to the basement membrane occurs following birth and spermatogonial stem cells (SSC) generate a stem cell pool which remain silent until puberty [reviewed by [8] [9]].

Following puberty, prespermatogonia consistently undergo mitotic division at the periphery of seminiferous tubules in testes. In mammals, the three types of spermatogonia are spermatogonia-type A, -intermediate, and -type B. While type-A spermatogonia

maintain spermatogonial stem cell population via mitosis, intermediate spermatogonia generate type B spermatogonia by meiosis in testis. Consequently, first primary spermatocytes, including leptotene, zygotene and pachytene spermatocytes are derived from type B spermatogonia. Then pachytene spermatocytes undergo meiosis I leading to secondary spermatocytes that will generate round spermatids via meiosis II. Finally, round spermatids generate elongated spermatids that will become spermatozoa [10]. The final stage of the spermatogenesis is called spermiogenesis where spermatozoon is being formed through a series of nuclear and morphological changes. While the acrosome is formed, DNA in the nucleus becomes condensed and histones (DNA binding proteins) are replaced by protamines. With a loss of most of its cytoplasm, a flagellum and mid-piece are developed in spermatozoon. Spermatozoa are delivered to the lumen of the seminiferous tubule and as they pass through the epididymis, progressive motility is gained. Final maturation is achieved by capacitation in the female reproductive tract [11].

From an endocrinology point of view, spermatogenesis is a hormone dependent cycle where gonadotropin releasing hormone (GnRH) is first released from the hypothalamus, which stimulates the anterior pituitary gland to secrete follicle-stimulating hormone (FSH) and luteinizing hormone (LH). Secretions of these two hormones affect different cell types in the testes; LH stimulates the Leydig cells to release testosterone and FSH promotes spermatogenesis by stimulating the Sertoli cells. In contrast to testosterone's role, sperm production is controlled by inhibin which blocks secretion of FSH secretion via a negative feedback mechanism [6]. Additionally, spermatogenesis is a stage-dependent process where numerous stages occur concurrently in a tubule. A spermatogenic cycle, from spermatogonia to mature spermatozoon, differs among species

and is completed in approximately 64 days with six stages in man, in approximately 68 days with twelve stages in bull, and in approximately 21 days with twelve stages in mouse [12].

DNA damage in sperm

As being transported outside of the body via ejaculation, spermatozoa are more susceptible to DNA damage compared to somatic cells. Damage to DNA in human sperm includes single strand (ss) DNA or double strand (ds) DNA breaks, the generation of abasic sites, DNA oxidation or alkylation, DNA-DNA or DNA-protein crosslinks, and DNA fragmentations [13]. When DNA is damaged in the cell, one or more than one response can be seen such as apoptosis (programmed cell death), transcriptional response, recruitment of DNA repair enzymes, activation of cell cycle checkpoints, and tolerating the damage. Usually, if the DNA damage in the cell is moderate, it can be repaired by DNA repair enzymes or spermatogenesis can be halted. Depending upon the severity of damage in the DNA, repair enzymes can fix the lesion. Alternatively, when extensive damage occurs in sperm DNA, the cells are eliminated by cell death mechanisms [13, 14].

Spermatozoa with intact DNA are essential for proper fertilization and the reproduction process in mammals. Hence, DNA damage in these cells would be detrimental for their offspring due to hereditary reasons. Fundamentally, there is a two-step hypothesis to explain how DNA damage may occur in sperm. In the first step, sperm DNA damage may occur during spermatogenesis via defective maturation such as impaired chromatin modeling and inefficient protamination; which will increase sperm vulnerability to any stress. Spermatozoa are exposed to several internal and external

factors such as changes in pH and temperature and excessive mitochondrial activity during their journey from the testis to the female reproductive system. This journey may cause oxidative stress (OS) generated by reactive oxygen species (ROS). In the second step of the two-step hypothesis this OS either triggers a death pathway, apoptosis, or directly causes oxidative DNA damage in the sperm, leading to DNA fragmentation [13]. Alternatively, nuclear DNA damage in mature human spermatozoa is explained by a three-mechanism theory. According to this theory, the first origin of DNA damage in sperm is any alterations in sperm chromatin packaging during spermiogenesis. The second reason why there are spermatozoa with DNA damage in ejaculated semen is due to abortive apoptosis. The third scenario is that the oxidative stress produced endogenously or exogenously, induces DNA damage in spermatozoa [1, 15, 16].

Sperm chromatin condensation

Chromatin condensation, also known as DNA packaging, is critical in sperm. There are three benefits to explain why DNA is more compact in spermatozoa compared to somatic cells. The first reason for this compaction is to optimize the sperm cell's shape that enables their motility through reproductive tracks in both the male and female. Another reason is that the nuclei of spermatozoa are protected by super-compaction from the effects of genotoxic factors. The third reason is that sperm compaction affects the imprinting of the paternal genes in fertilization regarding epigenetic reprogramming of the zygote. DNA in the sperm head is tightly packaged by arginine and cysteine rich nuclear proteins known as nucleoproteins that package DNA molecules over ten times more efficiently than nucleohistones [17]. While somatic cells package their DNA as a solenoid model, DNA in sperm becomes a loop represented as a doughnut (donut) model

or torus in mammals (See Figure 1.2 [18]). According to this model, mammalian sperm chromatin is first packaged into protamines and then coiled with approximately 50 kb of DNA into a compact donut shape, called protamine toroid. The protamine-DNA toroid then attaches to a proteinaceous nuclear matrix via matrix attachment regions (MAR) similar to somatic cells. However, there is a toroid-linker between MAR and protamine-DNA toroid in spermatozoa, which contains a piece of DNA packed by solenoids. Thus, DNA nicks generally occur in this toroid linker; indeed, endogenous DNase digests DNA at MAR regions [19] [20].

In the course of chromatin condensation taking place in spermiogenesis, the histones are firstly replaced by transition proteins (TP) and then protamines; in the meantime, DNA replication and RNA transcription are halted in the spermid stages. In detail, four core (canonical) histones in mammalian cells are H2A, H2B, H3, and H4 including H1 as a linker histone, and they are highly conserved among species in contrast to protamines. The histone core is an octamer containing 2 copies of each histone and forming a tetramer with H3 and H4, including 2 dimers of H2A/H2B. Histone gene families are classified into three groups; replication-dependent, replication-independent and tissue specific histones. For example, TH2A, TH2B, H3t, H4 and H1t linker are the testis-specific histones [21]. In contrast to H4, the remaining histones contain several subtypes or variants with different functions [22, 23]. For example in humans, the testis specific variant of H3 is H3t, while in mice it is H3.3A and H3.3B. Additionally, CENP-A and SubH2Bv histone variants have been identified in bovine sperm so far [24].

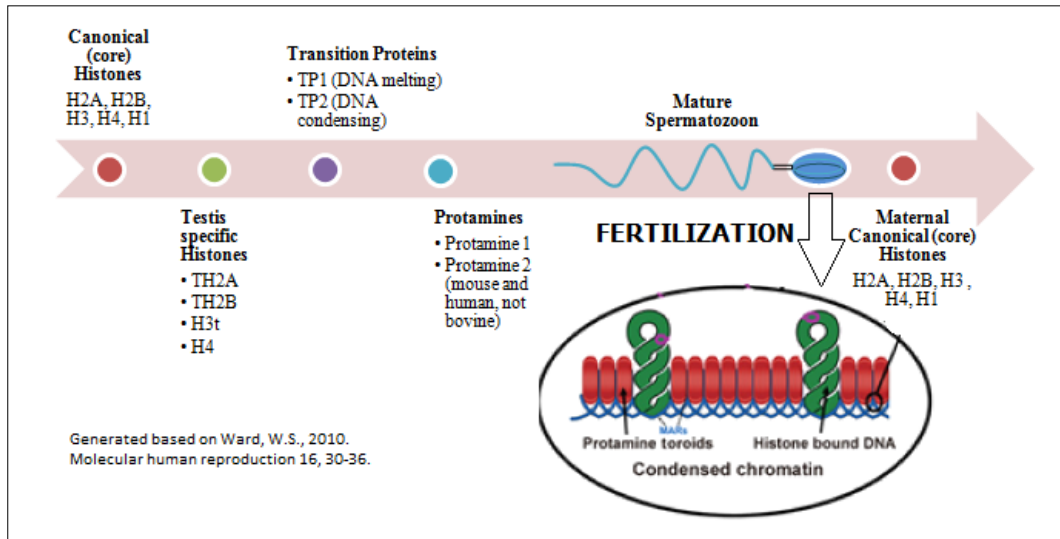


Figure 1.2 DNA Packing in Spermatozoa (revised from [18, 19]).

In contrast to histones, protamines differ among species. For instance, mature human sperm express protamine 1 (HP1), 2 (HP2) and 3 (HP3) [25] while mature mouse sperm possess protamine 1 (PRM1) and protamine 2 (PRM2) [26], and mature bull sperm chromatin is only packaged with protamine 1 (PRM1) [27, 28]. The distribution of these protamines in the genome varies in mammals. In humans, approximately 85% of DNA is packed with protamines containing equal amounts of PRM1 and PRM2 [26] while the remaining 15% is bound by histones [29]. However, protamines are not equally distributed in mice spermatozoa or one of the protamines becomes nonfunctional during spermatogenesis like bovine PRM2. Since mature bull spermatozoa have only PRM1, it is proposed as a model organism for studies on sperm chromatin modeling. Protamine 1 has three domains including an arginine (R)-rich central DNA binding domain and cysteine (C)-rich amino and carboxyl-terminal domains. Previously, PRM1 was shown to be part of intra- and inter-molecular disulfide bonds during DNA packaging [30]. It was

hypothesized that one PRM1 molecule rolls 11bp of DNA sequence, which is extremely tight compared to the histone core that wraps ~147bp of DNA [31].

Apoptosis

Apoptosis is a mechanism of programmed cell death and is genetically regulated by pro- and anti-apoptotic genes in the cell. Apoptosis works synchronously, but oppositely with mitosis and requires the activation of specific enzyme cascades to regulate cell proliferation in the animals [32]. Apoptosis may occur either physiologically or pathologically in the cell and perturbation of the mitosis/apoptosis balance is associated with many diseases.

Apoptosis is driven by three distinct phases referred to as induction, execution, and degradation and each of these stages activates a mitochondrial pathway. Mitochondria play two vital roles in the production of healthy sperm cells: (1) they provide ATP energy to support motility, and (2) they facilitate in the regulation of cell death. It has been found that mitochondria can sustain significant damage by ROS. Signals for the activation of apoptotic pathways can be either extrinsic, which are activated by tumor necrosis factor family receptors (TNF), or intrinsic, which are default pathways for cells that have been damaged due to stress caused by factors such as ROS or DNA damage. Extrinsic pathways involve the expression of pro-apoptotic factors, such as CD95 and TNF receptor 1, on the cell surface. Intrinsic pathways are used to initiate apoptosis from within the cell in response to cytotoxic stimuli and pro-apoptotic factors, such as cytochrome C and endonuclease G, which are released from the mitochondria and signal the activation of caspases. Caspases are a family of cysteine proteases that are an essential component in the process of apoptosis. Induction of apoptosis causes an

increase in the permeability of the mitochondrial membrane, resulting in decreased mitochondrial membrane potential ($\Delta\Psi_m$) and the release of pro-apoptotic factors, such as BAX, BAK, and PUMA. In the course of apoptosis, phosphatidylserine (PS) found on the inner leaflet of the plasma membrane are translocated to the outer leaflet. Translocation of PS triggers recognition by macrophages including phagocytosis by either macrophages or adjacent cells. However, when apoptosis increases in the cells and cannot be eliminated by the system, apoptotic cells with DNA-damage remain and lead to defects in the body [32] [33].

During spermatogenesis, apoptosis plays a key role in removing abnormal cells. In other words, spermatogenesis is controlled via apoptosis to limit the spermatozoa that can be supported by sertoli cells in the testis and to eliminate abnormal cells. However, how these apoptotic spermatozoa are formed remains unclear. It is believed that apoptosis occurs during either the pre-ejaculation [1] or post-ejaculation period [34]. In some cases, apoptosis is bypassed by anti-apoptotic factors, endogenously or exogenously. Thus, some spermatozoa may escape apoptosis without tagging apoptotic markers during proliferation and their DNA still remain damaged at the end of maturation, which is called “abortive apoptosis” [15]. Therefore, the semen may include significant numbers of damaged and immature spermatozoa, which is one of the reasons for the presence of damaged DNA in mature spermatozoa (Figure 1.3).

Oxidative stress

In the cell, there is a critical balance between the ROS and antioxidant capacity. When this balance is changed, the cell is exposed to OS, which leads to oxidative DNA damage [35]. Free radicals are constantly produced as metabolites in normal aerobic

organisms; however, the oxygen-mediated ones are radical and the increased levels of these oxygen-mediated radicals can be vital for the cells. Certain concentrations of ROS are generated via oxidative phosphorylation in the mitochondria. Two major oxygen radicals in the cells are superoxide radical ($O_2^{\bullet-}$) and hydroxyl radical ($\bullet OH$). In addition, hydrogen peroxide (H_2O_2) is also a ROS because of its highly oxidizing capacity; however, it is not a true radical.

In spermatozoa, the origin of oxidative stress can be either intrinsic or extrinsic. Intrinsic factors of OS include smoking, varicocele, age, radiation, chemotherapy, alcohol and caffeine [36, 37]. Extrinsic factors are associated with assisted reproduction techniques (ART) and include sperm isolation techniques, sperm cryopreservation, centrifugation [38] [35, 39]. Although increased ROS in spermatozoa is considered toxic, lower levels of ROS are essential for motility, hyperactivation, capacitation, the acrosome reaction, and fertilization. Two major features in spermatozoa to protect the DNA from free radicals are DNA packaging and seminal plasma. Seminal plasma contains antioxidants such as superoxide dismutase, catalase, and glutathione peroxidase/ glutathione reductase in addition to non-enzymatic antioxidants such as ascorbic acid, vitamin E, pyruvate, albumin, taurine, hypotaurine, ubiquinol, vitamin A and urate. These antioxidants play a role in the protection of spermatozoa from ROS-induced damage including the prevention of DNA damage [5, 35, 40].

Detection of DNA damage in sperm

Sperm DNA damage is determined using several techniques in mammals. By detecting the DNA damage in spermatozoa, the origin of the damage can also be evaluated. Some methods rely on the maturity of spermatozoa; for instance, toluidine

blue and aniline blue staining detect the sperm DNA binding proteins in histones and protamines. In addition to maturity, DNA breaks can also be observed in spermatozoa using TdT-mediated-dUTP nick end labeling (TUNEL) assay where fluorescence probes bind to DNA breaks. This method that can be utilized either with fluorescence microscopy or by flow cytometry to measure ssDNA -dsDNA breaks, DNA integrity and DNA fragmentation at the same time. However, using TUNEL is not sufficient to distinguish between ssDNA and dsDNA breaks in the cell. On the other hand, in-situ nick translation or fluorescence in situ hybridization (FISH) assays can be used to identify only ssDNA breaks. The latter method is also designed to localize the specific DNA sequences on the chromosomes. Additionally, ssDNA breaks can be distinguished from dsDNA breaks by acridine orange (AO) stain where AO stain is combined with the flow cytometry technique, which is called sperm chromatin structure assay (SCSA) [35]. In addition to maturity and DNA breaks, the integrity of sperm chromatin can also be assessed by sperm chromatin decondensation (SCD) assay, including the newly developed Halosperm test for human [35] [41] or Halomax for animals [42]. Another method to detect DNA damage in sperm is the single-cell gel electrophoresis (Comet) assay. While the neutral COMET can identify dsDNA breaks, the alkaline COMET can detect both ssDNA and dsDNA breaks [43]. In addition to these techniques, oxidative DNA damage caused by oxidative stress can be detected using eight-oxo-2'-deoxyguanosine (8-oxoG), a marker of oxidative DNA damage by high-performance liquid chromatography. The aforementioned techniques were used to detect sperm DNA damages in the studies where some of the results were correlated with male infertility [44] [45] [35] [46].

Justification of the study

Although male infertility makes up 25% of infertile couples [5], mechanisms of male infertility not have been studied as extensively as female infertility. Conventional semen analysis was shown to be insufficient to predict reproductive outcomes in both animals and humans. In animals, compensatory fertility can be improved by increasing the amount of spermatozoa; however, non-compensatory fertility is caused by molecular defects in sperm and results in sub-par fertility [47]. Molecular defects, especially damage to DNA, in mammalian sperm were demonstrated to be essential in sperm physiology in humans [1, 48-51], bulls [52-55], and mice [56, 57]. Studies over the past 40 years suggest that sperm chromatin alterations (such as DNA fragmentation induced by either chromatin condensation errors, apoptosis and/or oxidative stress) might be negatively associated with fertilization and early embryonic development [1, 2], [3] [4], and they may also be related to field fertility of bull semen [58]. Immature spermatozoa with histone-packaged chromatin are more susceptible to DNA damage than the mature sperm with protamine-packaged. In addition, it was identified that sperm DNA damage is negatively associated with fertilization rate, implantation, successful pregnancies [1-3], higher occurrences of miscarriage [4], and is also related to field fertility of bull semen [58]. On the other hand, other groups established that DNA damage of sperm was not related to male fertility [43, 59-63]. Studies demonstrated that increased levels of apoptotic spermatozoa have a direct influence or impact on poor bull fertility by decreasing sperm viability [52-54]. In addition to errors concerning chromatin condensation, male infertility was established to be associated with the ratio of histone-retention as well as protamine-condensation, mostly in human spermatozoa For example,

some studies focused on the determination of a ratio between protamine1 and 2 in infertile men compared to their fertile counterparts [25, 29, 64, 65], while others revealed a relative amount of histone over protamines [66]. However, what we do not know is to what extent sperm DNA compaction influences male infertility. Since the origin of DNA damage in sperm and its relationship with male infertility is still unsettled, details of mechanisms causing DNA damage as well as the specific effects of damaged DNA on fertility largely remains unclear. Despite the importance of male infertility, there are no reliable molecular biomarkers to determine semen quality and bull fertility. Therefore, this study focused on the investigation of the origin of DNA damage in bull sperm and its relationship with male infertility

CHAPTER II
INTERRELATIONSHIPS BETWEEN APOPTOSIS AND FERTILITY IN BULL
SPERM

Abstract

Male fertility, the ability of sperm to fertilize and activate the egg and support early embryogenesis, is vital for mammalian reproduction. Despite producing adequate numbers of sperm with normal motility and morphology, some males suffer from low fertility whose molecular mechanisms are not known. The objective was to determine apoptosis in sperm from high and low fertility bulls and its relationship with male fertility. DNA damage, phosphatidylserine (PS) translocation, and expression of pro- and anti-apoptotic proteins (BAX and BCL-2) in the sperm were determined using TUNEL, Annexin V, and immunoblotting approaches, respectively. Amounts of apoptotic spermatozoa were 2.86% (± 1.31) and 3.00% (± 0.96) in high and low fertility bulls, respectively ($P=0.548$), and were not correlated with fertility. There was a negative correlation between early necrotic spermatozoa and viable spermatozoa ($r = -0.99$, $P<0.0001$). Fertility scores were correlated with live spermatozoa detected by an eosin-nigrosin test and necrotic spermatozoa determined via flow cytometry ($r = -0.49$, $P<0.006$ and $r = -0.266$, $P<0.0113$, respectively). BAX expression was similar among groups although there was a variation (Bull 1–3 vs. Bull 4–5) in the low fertile group

($P < 0.283$). BCL-2 was not detectable in any of the sperm samples. The results shed light on the molecular and cellular underpinnings of male fertility.

Key words: Apoptosis, DNA damage, Male infertility, Sperm

This study has been published: Citation Dogan, S., et al., Interrelationships between Apoptosis and Fertility in Bull Sperm. [J Reprod Dev, 59(1): 18-26, 2013. ISSN 1348-4400 (Electronic)]

Introduction

The quality of paternal DNA transmitted through sperm is an important factor for maintaining the reproductive potential of males, fertilization, embryonic development, and beyond [67, 68]. Apoptosis or programmed cell death is a major factor proposed to cause DNA damage in spermatozoa [49, 69] before and after spermatogenesis. Apoptosis naturally removes unnecessary or damaged cells and contributes to the maintenance of homeostasis in tissues; [49, 69] indeed, abnormal apoptotic processes might result in abnormal sperm development [1]. Stages of induction, execution, and degradation [54] as well as signaling pathways of intrinsic and extrinsic origin are involved in apoptosis (Figure 2.1). Signals for the extrinsic pathway are activated by receptors from the tumor necrosis factor family (TNF), and signals for the intrinsic pathway are triggered by factors such as oxidative stress and nuclear or mitochondrial DNA damage [1, 4].

Apoptosis is one of the well-known cell death mechanisms with necrosis and it is regulated by several genes and molecules that all play a large role in the initiation of apoptosis, such as BAX, BAK, PUMA, p53, c-Myc and BCL-2 (the B-cell lymphoma/leukemia 2) family members that consist of pro- and anti-apoptotic factors (See [70] for further information) which also trigger other caspases [4, 52, 54, 71].

Activation of BAX/BAK1 proteins trigger the release of cytochrome c and other apoptogenic factors from the mitochondria leading to apoptosome formation, which then activates caspase-9 with caspase- 3 and 7 [4]. In the course of apoptosis, a translocation of PS from the cell membrane occurs on the surface of apoptotic cells recruiting the neighboring macrophages for phagocytization; which is the main difference from necrosis [52, 53]. Sperm DNA damage induced by apoptosis has been demonstrated by several research groups in different mammals: human [1, 48-51]; bovine [52-55]; and murine [56, 57]. The balance between germ cells and sertoli cells in the testes during spermatogenesis is maintained by apoptosis and an imbalance in this process was shown to cause infertility in males [4].

Mechanisms of male infertility have not been researched as extensively as female infertility and have only become of major interest within the last two decades. There is still a significant gap in the knowledge base of these mechanisms and their relationship to sperm DNA damage and apoptosis. It has been found that increases in apoptotic spermatozoa have a direct influence or impact on poor bull fertility by decreasing sperm viability [52-54]. Conventional semen analysis has proven to be a poor predictor of reproductive outcomes and seems to be testing subjective rather than quantitative evaluations of male fertility.

Studies have shown that sperm DNA damage is negatively associated with fertilization rate, implantation, successful pregnancies [1-3] ,higher occurrences of miscarriage [4], and is also related to field fertility of bull semen [58]. However, contrary results have been reported by others [43, 59-63]. Since this relationship is still unsettled, details of mechanisms causing DNA damage as well as the specific effects of damaged

DNA on fertility largely remains unclear. Despite the importance of male infertility, there are no reliable molecular biomarkers to determine semen quality and bull fertility. The purpose of this study was to determine apoptosis in sperm from bulls with varying fertility and to determine to what extent DNA integrity is linked to bull fertility. In addition, we investigated if apoptotic proteins could be the best biological marker(s) that could estimate the fertility score for males. Is determination of apoptosis really necessary to predict the sperm DNA integrity and male fertility? Instead of apoptosis determination, what kind of test could be cost-effective? This study focused on the investigation of the apoptosis paradox concerning why different bulls are able to provide similar numbers of sperm cells with normal morphology, motility and viability, and yet have differences in fertility.

Material and Methods

All chemicals and reagents are stated or are otherwise supplied from Sigma (MO, USA). The experimental design of this study is presented in Figure 2.2.

Determination of bull fertility

In this study, we used sperm from bulls that produce abundant amounts of sperm with normal motility and morphology. Thus, this study addresses so called “non-compensatory fertility” where it is thought that molecular defects in the sperm cause sub-par fertility [47]. In the Alta Advantage Program (Alta Genetics, Watertown, WI, USA), fertility of bulls are predicted quarterly using updated data from partnering herds as described in [72]. The list of the bulls and fertility phenotypes used in this study is shown in Table 1. The environmental and herd management factors that influence the fertility

performance of the sires are adjusted using threshold models which are similar to previously published models by Zwald *et al.* [73], [74]. Estimation of parameters and fertility prediction were obtained using Probit F90 software [75]. The outcome of each breeding event and the environmental factors, such as the effects of herd-year-month, parity, cow, days in milk, and sire proven status are adjusted. Afterwards, the fertility of each sire was expressed as the percent deviation of its conception rate from the average conception of all bulls in the database with at least 300 breeding outcomes. For this study, we used the standard deviation (SD) of the population as the criterion to classify bulls as high and low fertility. Bulls having 2 SD above the average were considered as high-fertility, and those that are 2 SD below the average were considered as low-fertility. Thus, the fertility differences between high and low fertility groups were 4 SD which can be considered extreme outliers for the given population. Additionally, bulls were required to have a minimum of 500 breeding records to be qualified for higher reliability.

Isolation of spermatozoa

Cryopreserved semen samples of ten bulls (three straws from three ejaculates per bull) with varying fertility were provided by Alta Genetics. The samples were thawed and for each bull, the total spermatozoa collected were purified by Percoll gradient centrifugation according to [72] with minor changes. Briefly, spermatozoa were isolated by using 45% Percoll prepared with 90% Percoll and phosphate-buffered solution (PBS; Gibco, Invitrogen, Carlsbad, CA, USA) at 700 x g for 15 min to only remove the cryopreservation extender, sperm pellets were then washed with PBS at 700 g for 10 min. Using this method, sperm population was not selected based on motility or morphology. This is consistent with previous studies where this approach does not allow sperm

selection to take place based on their viability, motility or cell integrity [76]. Cell numbers were determined using a hemacytometer and cell concentration in warmed PBS was adjusted to 5×10^5 /ml for Annexin V assay (Annexin-V-FLUOS Staining Kit, Roche Applied Science, Indianapolis, IN, USA) and 1×10^6 /ml for TUNEL assay (In Situ Cell Death Kit, Roche Diagnostics, Indianapolis, IN, USA). All centrifugations were performed at room temperature and spermatozoa were stored in an incubator at 37 °C prior to Annexin V and TUNEL assays to avoid oxidative shock and to maintain the accuracy of results.

TUNEL Assay

Following isolation of spermatozoa, the sperm pellets were washed twice in PBS with 0.1% Bovine Serum Albumin [77] and suspended in 100 µl of PBS/0.1 % BSA. The pellets were then fixed in 100 µl of 4% paraformaldehyde at room temperature for 60 min, re-suspended in 100 µl of PBS and then permeabilized in 100 µl of 0.1% Triton X-100 in 0.1% sodium citrate in PBS on ice for 2 min. While the ten individual pellets were being fixed and permeabilized, the TUNEL reaction mixture was prepared by removing 100 µl of label solution for two negative controls and adding the total volume (50 µl) of enzyme solution to the remaining 450 µl label solution to obtain 500 µl TUNEL reaction mixtures. The negative control was incubated, fixed and permeabilized in 50 µl of label solution without the TdT enzyme, while the positive control was incubated, fixed and permeabilized with DNase 1 (100 IU, Invitrogen, Carlsbad, CA, USA) at 25 °C for 10 min. Next, the pellets were washed twice with 200 µl of PBS/0.1% BSA and then re-suspended in 50 µl TUNEL reaction mixture; including the positive control. Once the TUNEL reaction mixture had been added, the samples were incubated at 37 °C in the

dark for 60 min. The samples were then washed with 200 μ l of PBS/0.1% BSA, placed into a transparent tube with a final volume of 400 μ l in PBS and were immediately analyzed by flow cytometry (FACSCalibur, BD Biosciences, San Jose, CA, USA). The TUNEL assay was observed using fluorescence microscopy (Axiovert 200 M Inverted Research microscope, Zeiss, Göttingen, Germany) prior to flow cytometry to determine to what extent the assay has worked. The data were then expressed in a flow-cytometric plot. All experiments were repeated three times by using three experimental replicates (n=90; 9 different reads per bull).

Annexin V assay

For the Annexin V assay, Annexin-V-FLUOS Staining Kit (Roche Applied Science, Indianapolis, IN, USA) was used according to the manufacturer's recommendations. Briefly, Annexin-V-FLOUS labeling solution was prepared by combining 20 μ l of AnnexinV-Flous labeling reagent and 20 μ l of propidium iodide (PI). Next, the isolated sperm samples were re-suspended in 100 μ l of AnnexinV-Flous labeling solution at 37 °C. This mixture was then incubated at room temperature in the dark for 10 min. Following incubation, 400 μ l of incubation solution was added to each sample and analyzed using the flow cytometer. A flow-cytometric plot of frozen-thawed sperm following Annexin V assay is represented in Figure 2.3. Annexin-V/PI assay distinguishes four different subpopulations of cells, as indicated in the related figure. Among the population of spermatozoa, late necrotic spermatozoa were stained with PI, but not with Annexin V whereas early necrotic spermatozoa were labeled with both Annexin V and PI. Viable spermatozoa were stained by neither Annexin V nor PI, while apoptotic spermatozoa were labeled only by Annexin V, but not by PI. In order to

confirm sperm cell viability, 10 μ l of sperm suspension was mixed with 10 μ l of eosin-nigrosin staining solution to prepare a smear slide according to [78]. Eosin stains the post-acrosomal region of spermatozoon while nigrosin penetrates into the acrosome. They are usually used together to better evaluate spermatozoa via light microscopy [79]. A total of 100 sperm cells per slide were counted under light microscope. All experiments were repeated three times by using three experimental replicates.

Isolation of sperm proteins

Sperm cells were isolated according to the protocol listed above and washed with PBS containing protease inhibitor cocktail (Roche Applied Science) to avoid protein degradation, and then stored at -80°C until protein isolation. Spermatozoal proteins were extracted using SDS sample buffer containing 66 mM Tris-HCl (pH 6.8), 26% glycerol, and 2% SDS. Next, 5 μ l of β -Mercaptoethanol was added fresh to 95 μ l of SDS sample buffer. The sperm pellets were then re-suspended in the above mixture, vortexed for 30 sec followed by boiling the samples for 10 min. The samples were then cooled on ice for two min prior to centrifugation at 4°C and 700 g for 10 min. The supernatant containing the proteins were then diluted by ddH₂O [1:100] and quantified using microBCA protein assay based on the bicinchoninic acid assay (Thermo Scientific, Rockford, IL, USA) method according to the manufacturer's recommendations.

Immunodetection of apoptotic proteins

Equal amounts (5 mg/well) of the isolated proteins were loaded from Bull 1 to 10 based on their fertility scores and separated in 10% SDS-polyacrylamide gels [80], and then were transferred onto polyvinylidene fluoride (PVDF) membranes by the semi-dry

transfer method using HEP-1 Semidry Electroblotting (Thermo Scientific). The membrane was then blocked with 1xTris buffered saline with 1% casein for 60 min (Bio-Rad, Hercules, CA, USA) at room temperature and incubated with primary antibodies, BAX (N-20) and BCL-2 (N-19) (sc-493 and sc-492 from Santa Cruz, Santa Cruz, CA, USA) at 4 °C overnight with the dilutions of 1:1000 and 1:250, respectively. Beta-tubulin (N-20) (sc-9935 from Santa Cruz, Santa Cruz, CA, USA) was used as a loading control for each primary antibody at a dilution of 1:500. The next day, the membrane was washed three times at room temperature for 15 min with washing buffer containing 0.1% Tween20, followed by incubation with secondary antibodies conjugated to horseradish peroxidase (Donkey anti-rabbit IgG-HRP, sc-2313 for BCL-2 and BAX and donkey anti-goat IgG-HRP, sc-2020 for β -Tubulin from Santa Cruz, Santa Cruz, CA, USA) at room temperature for 60 min. Following washing, chemiluminescent substrate (WBKLS0500, Millipore, Billerica, MA, USA) was added to the membrane to detect the binding of the antibodies. We used a protein marker (EZRun Protein Marker, Fisher Scientific, Pittsburgh, PA, USA) to estimate the size of the proteins of interest. The antibodies were tested prior to their use. Specifically, testis tissue was used as positive control while incubation of the membranes without the primary antibody was utilized as a negative control for each protein. Following immunoblotting, the intensities of the bands were quantified using Image Lab software (Bio-Rad, Hercules, CA, USA).

Statistical analysis

Data were obtained from three different trials with three technical replicates for apoptosis and TUNEL experiments, with two technical replicates for eosin-nigrosin test and without technical replicates for western blotting. In other words, nine, six and three

measurements per bull were used for data analysis from the apoptosis and TUNEL experiments, eosin-nigrosin test and western blotting, respectively. All percentage data was first verified to be normally distributed by the Shapiro-Wilk test and Kolmogorov-Smirnov (K-S) test using PROC UNIVARIATE command in SAS Version 9.2 for Windows (SAS Institute, Cary, NC, USA). Total numbers of measurements were then classified into two groups, high and low fertility bulls, and then analyzed using the one way ANOVA test with PROC ANOVA command in SAS, including mean values (\pm SD). Since we designed the experiments based on the 3 \times 3, 3 \times 2 and 3 replicates per bull for the apoptosis and TUNEL experiments, eosin-nigrosin test and western blotting, respectively, we analyzed the data using the ANOVA test. Overall relation among the data was performed using Pearson correlation analysis with PROC COR command in SAS, determining any significant ($\alpha \leq 0.05$) linear associations between fertility, necrotic spermatozoa, early necrotic spermatozoa, viable spermatozoa, apoptotic spermatozoa, live spermatozoa, dead spermatozoa, spermatozoa with DNA fragmentation, and BAX regardless of any grouping. Following a stepwise multiple regression analysis using PROC GLMSELECT command in SAS, the regression analysis of the selected variables was performed by PROC REG to determine which combination of measured variables might best predict fertility.

Results

All parameters that were used for analysis are listed in Table 2.1 and Pearson correlation coefficients are shown in Table 2.2.

Fertility differences among the bulls

The fertility data were determined as the SD from average fertility values of around 1,000 bulls. Fertility results of five high and five low-fertility bulls are summarized in Table 1. The average fertility index of high and low fertility groups were $6.14 \pm 1.1\%$ and $-9.94 \pm 3.6\%$ of the average (Zero=0), respectively. The ranking of the bulls was done using their fertility scores obtained from the company, which was explained in the method section. Briefly, the average of fertility was assigned to be zero=0; thus, above this value was considered high fertility and defined as positive values while below average was defined as negative (-) values and named as low fertility bulls. This allowed us a unique group of samples which had 16.08% fertility difference between high and low fertility groups. The average number of inseminations for the high and low fertility groups were 881.8 ± 303.3 and 1056.2 ± 371.2 , respectively (Mean \pm SD) (Table 2.1).

Extent of DNA damage in sperm

Spermatozoa with DNA fragmentation were detected using flow cytometry. The percentage of sperm with TUNEL positive (DNA damaged) in high and low fertility bulls was 3.51 ± 2.23 and 3.61 ± 2.20 , respectively; there was no significant difference between the two groups (P=0.826) (Table 2). According to our Pearson test results, DNA fragmentation was not correlated with fertility scores ($p > 0.05$). Likewise, DNA fragmentation detected by TUNEL assay was not correlated with the percentage of viable spermatozoa, necrotic, early necrotic and apoptotic spermatozoa detected by Annexin V assay (Table 2.2). The TUNEL assay was established by fluorescent microscopy prior to flow cytometry and spermatozoa with and without DNA fragmentation are shown (Figure

2.4). As a nuclear stain, DAPI was performed and DNA fragmented spermatozoa were stained green compared to those that were stained blue (DAPI), which represented spermatozoa with non-fragmented DNA.

Detection of apoptosis via annexin V

The flow cytometric plots of spermatozoa from two bulls with different fertility are shown in Figure 2.5; [bull K_1.002 (Bull 1) is low fertility and bull E_3.031 (Bull 10) is high fertility]. The percentage of apoptotic spermatozoa in high and low fertility bulls was 2.86 ± 1.31 and 3.00 ± 0.96 , respectively; there is no significant difference between groups ($P=0.548$). In addition to apoptotic spermatozoa, the percentages of necrotic, early necrotic and viable spermatozoa in high and low fertility bulls were $3.48 (\pm 1.59)$, $31.04 (\pm 9.27)$, $62.62 (\pm 9.1)$ and $4.13 (\pm 1.86)$, $32.13 (\pm 9.26)$, $60.72 (\pm 8.51)$, respectively. There was no significant difference of necrotic, early necrotic and viable spermatozoa between groups ($P=0.079$, 0.579 and 0.311 , respectively) (Table 2.1). There was a negative correlation between early necrotic spermatozoa and viable spermatozoa detected via flow cytometry ($r = -0.991$, $P < 0.0001$). In addition, apoptotic spermatozoa showed a positive correlation with early necrotic spermatozoa ($r = 0.358$, $P < 0.01$), whereas a negative correlation existed with necrotic spermatozoa and viable cells ($r = -0.688$, $P < 0.0001$; $r = -0.367$, $P < 0.05$, respectively) (Table 2.2). The eosin-nigrosin test was done to confirm flow cytometric data and its results were indicated as alive sperm in the data (Tables 2.1 and 2.2, respectively). Two microscopic slides of eosin-nigrosin stain from two different bulls are shown in Figure 2.6; live spermatozoa were not stained while dead spermatozoa were labeled with the stain. A live cell population in high and low fertility bulls was $59.27 (\pm 8.61)$ and $52.60 (\pm 7.06)$ and this difference was significant ($P < 0.01$)

in Table 2.2. In addition, the data demonstrated a positive correlation with viable cells and a negative correlation with early necrotic spermatozoa detected by flow cytometry ($r=0.386$, $P<0.04$; $r=-0.435$, $P<0.02$, respectively). There was a negative correlation between live spermatozoa detected by eosin-nigrosin test and fertility score, and this was statistically significant ($r=-0.49$, $P<0.05$). No correlation between apoptosis and DNA fragmentation existed.

Detection of apoptotic proteins via immunoblotting

The expression of BAX (pro-apoptotic), but not of BCL-2 protein (anti-apoptotic) was determined using WB. The signal intensities from the expressed proteins among bulls were determined by Image Lab software (Bio-Rad) and normalized using the internal control, β -Tubulin (BAX/ β -Tubulin). The size of BAX, BCL-2 and β -Tubulin bands appeared to be around 23-kDa, 26-kDa and 55-kDa based on the protein marker. The expressions of BAX among bulls in high and low fertility bulls were $2.47 (\pm 0.72)$ and $3.36 (\pm 3.23)$, respectively. The expression of BAX did not differ between groups ($P=0.283$) (Table 2.1). It was shown here that BAX was not correlated with fertility ($r=-0.301$, $P<0.12$). The distribution of western blotting data among the high vs. low fertility groups can be seen in Figure 2.7. The intensities of the protein bands detected via western blotting are analyzed for their distribution in each group. Any correlation between protein expression and other parameters were determined. The expressions of BAX, BCL-2 and β -Tubulin among the bulls were shown in Figure 2.7A. Testis sample from a bull with unknown fertility for each antibody was previously tested as a positive control to confirm the specificity of both antibodies, which was represented in Figure 2.7B. The negative control of western blotting experiments for both antibodies (BAX and BCL-2) where the

only secondary antibodies (donkey anti-goat IgG-HRP) were used is represented in the Figure 2.9.

A stepwise multiple regression analysis with fertility as a dependent variable and the seven other variables as predictive independent variables found a significant regression ($p < 0.06$) using two predictor variables (necrotic spermatozoa detected by flow cytometry, alive spermatozoa determined via eosin-nigrosin stain).

Discussion

The significance of damaged DNA in sperm is still debated as it may or may not be correlated with male fertility [4]. In this study, we used a bovine model to identify molecular markers and mechanisms regulating male fertility because there is a wealth of reliable information on bull fertility phenotypes derived from a thousand breedings and significant similarities exist between reproductive physiologies and genomes of bovine and human. Since we obtained semen straws from the company with their reliable fertility scores based on not only the semen quality of these bulls, but also their breeding scores to calculate their fertility scores, the bull's fertility scores were accurate and within a normal range, which were confirmed by a previous study [47].

In the course of apoptosis, BCL-2 anti-apoptotic and BAX pro-apoptotic proteins provide a signaling pathway that helps maintain the balance in a cell. In addition to caspases and other apoptotic enzymes, the relative amounts of these two groups of proteins are essential for whether the cell survives or undergoes apoptosis [81]. During spermatogenesis, BAX-mediated apoptosis serves as a checkpoint for maintaining the number and quality of spermatozoa. Also, it was demonstrated that BAX-deficient mice were sterile because of disordered maturation reflected by the absence of mature

spermatocytes and the presence of pre-meiotic cells with an atypical distribution of decondensed chromatin [82]. A similar study by Martin *et al.*, [54] also showed the expression of *Bax*, but not *Bcl-2* in cryopreserved bovine spermatozoa. As was shown here, BAX protein was present in bull sperm while the BCL-2 was not detected [54]. For the BCL-2 western blotting, we used the same antibody used against BCL-2 in monkey testis. [83], and in human testis [84]. We also confirmed the expression of BCL-2 protein in bull testis as a positive control; therefore, we are confident that this antibody was specific enough to detect BCL-2 in bull spermatozoa if it would be present. Furthermore, no cross-reaction was detected. In our study, BAX expression was not different between high and low fertility groups, and there was not any correlation between male fertility and the expression of BAX protein. Bulls 1–3 in the low fertility group displayed variations compared to bulls 4 and 5 in the same group and also bulls in the high fertility group. We demonstrated the distribution of BAX among bulls in Figure. 2.8, in which the variations of BAX can be seen. One reason for these variations might be the differences in response to the cryo-damage within individuals during cryopreservation.

In addition to apoptotic proteins, DNA damage and PS translocation were determined using flow cytometric assays in our study. These assays were specific enough to evaluate apoptosis and to distinguish it from necrosis in frozen bull spermatozoa based on the literature [2, 52]. According to another study, spermatozoa undergo apoptosis during the incubation time followed by swim-up; thus, the viable cell population in that study is less than what was observed in our study [55]. The correlation of fertility with DNA damage detected by TUNEL and PS translocation identified by Annexin V was significant in fresh bull sperm, but not in frozen samples, which was also supported by

others [52]. In contrast to a study, our results revealed that male infertility was not correlated with PS translocation in bulls [2]. According to another study, $1.2\% \pm 0.7$ of spermatozoa derived from two fertile bulls were TUNEL labeled concluding that bull sperm were resistant to the induction of caspase-mediated apoptosis following ejaculation [85], which was supported by our study. It was revealed that eosin-nigrosin stain was able to detect sperm vitality in bulls, and after thawing less than 50% of spermatozoa could survive [78]. Spermatozoa might be damaged by “cryo-shock” or “cold shock” containing possible damages to plasma, outer acrosomal membrane, or the acrosome and nucleus during cryopreservation. However, in regards to our own project, all of our samples were cryopreserved so that each sample was treated the same. Due to the cryopreservation of all of our samples our results are still objective because there was no mixture or comparison between cryopreserved and fresh samples.

Unlike our results, DNA fragmentation in sperm was significantly associated with fertility while evaluating the sperm quality in relation to fertility after artificial insemination (A.I.) [58]. Additionally, a study concluded that there was a significant negative correlation between male fertility and sperm DNA damage [3]. On the other hand, we suggest that there is no correlation between sperm DNA damage and fertility, which is supported by other studies [43, 59-61]. The lack of correlation between DNA fragmentation and fertilization rate was shown in their overall study, but suggested that different techniques such as intra cytoplasmic sperm injection (ICSI) and *in vitro* fertilization (IVF) may have influence as to how significantly DNA damage can affect fertility rates [63, 86].

In this study flow cytometry was used to quantitatively analyze spermatozoa and the potential nuclear DNA damage induced by apoptosis. Therefore, the quality and quantity of our results are more accurate due to the use of flow cytometry compared to conventional fluorescent microscopic methods. In addition to flow cytometry, our study is innovative by virtue of sufficient technical replicates per bull and their strong fertility data. The sperm gradient isolation method provides a selection of immature spermatozoa mostly with DNA damage compared to the use of whole semen, which may cause a bias in the results. According to a recent study, semen processing by density gradient centrifugation is useful in selecting sperm with better double-strand DNA integrity. In this study, the DNA fragmentation index [87] for whole semen (without Percoll isolation) was more than 30% compared to the DNA fragmentation index (DFI) of spermatozoa separated by 50% of a gradient solution [88]. This is unlikely in our study since we used 45% of gradient solution; sperm with DNA fragmentation detected by TUNEL was about less than 5% of the whole cell population. According to the previous studies, use of a 45% of gradient solution approach does not allow the sperm selection according to their viability, motility or cell integrity [76].

Since neither intrinsic nor extrinsic apoptotic pathways in sperm were the focus of our study, any speculations on the origin of DNA damage cannot be obtained. Since cryopreserved sperm is still being used for A.I. in the field, the current study focuses on frozen sperm rather than fresh semen. Cryopreservation affects sperm motility, vitality and its DNA integrity, as well as leading to increases in intracellular Ca^{2+} concentrations which leads to the release of pro-apoptotic factors in the cytoplasm. Therefore, nearly 50% of spermatozoa are dead after freezing and thawing, which is called the cryo-

survival rate [71], and this percentage is considered common in bull sperm [78]. The apoptotic cell population was determined to be less than 10% in our study because only cryopreserved spermatozoa were used and 50% of the cell population was already dead prior to the detection of DNA damage induced by apoptosis. However, a number of studies have determined the implications of cryopreservation and other stress responses of animals during spermatogenesis in affecting apoptosis-like events in sperm [89-91].

In conclusion, our results determined that the most relevant fertility markers might be the percentage of necrotic spermatozoa detected by flow cytometry and live spermatozoa determined via eosin-nigrosin staining and that there is no relationship between apoptosis and male fertility. None of the apoptotic variables were determined as a fertility marker in this study, so apoptotic markers may not be considered accurate indicators of fertility. Overall, apoptosis might be induced during spermatogenesis, and sperm cells rapidly undergo necrosis opposed to apoptosis following cryopreservation. Unlike apoptosis, necrosis might be the main pathway that influences sperm viability after thawing. Thus, further clinical studies should be performed to determine the molecular mechanism of the intrinsic apoptotic pathways, including the expression and roles of apoptotic proteins.

Acknowledgements

The funding of this study was provided by Mississippi Agricultural and Forestry Experiment Station and by Alta Genetics, Inc.

Table 2.1 Fertility Differences among the bulls

Bull	Group	Number of Breeding	% Fertility Deviation From Average
1	Low Fertile Bulls	1134	-14.7
2		769	-9.1
3		1671	-8.1
4		888	-7.2
5		819	-5.6
Mean		1056.2 ± 371.2	-8.94 ± 3.6
6	High Fertile Bulls	560	5
7		594	5
8		1222	5.1
9		1138	5.6
10		895	6.2
Mean		881.8 ± 303.3	5.38 ± 0.5

List of bulls and their fertility scores according to Alta Genetics data base including bulls' breeding numbers. Bulls are listed according to their fertility scores where Bulls 1–5 and Bulls 6–10 represent low and high fertility groups, respectively.

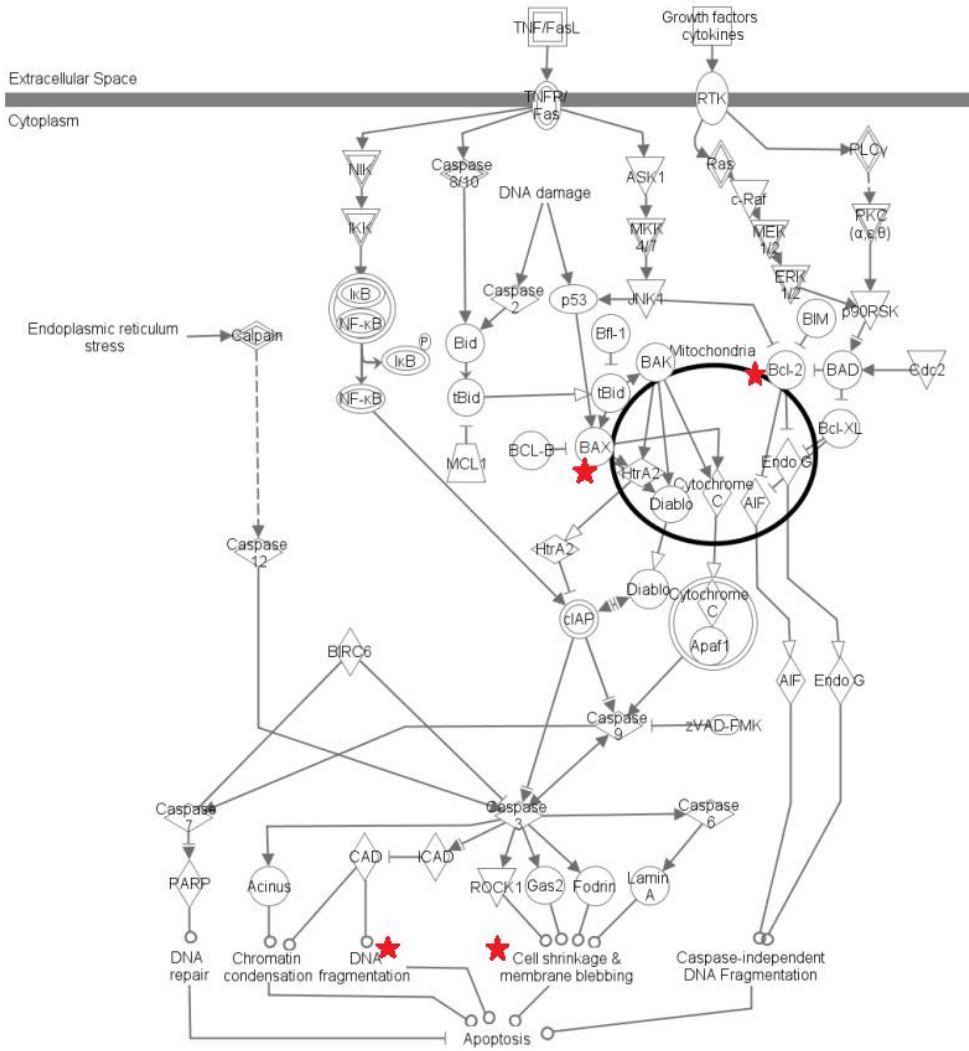
Table 2.2 Comparison of two groups (high vs. low fertility)

Parameters	High (Mean ± SD)	Low (Mean ± SD)	p-value
Necrotic spermatozoa (%)	3.48 ± 1.59	4.13 ± 1.86	0.079
Early necrotic spermatozoa (%)	31.04 ± 9.27	32.13 ± 9.26	0.579
Viable spermatozoa (%)	62.62 ± 9.1	60.72 ± 8.51	0.311
Apoptotic spermatozoa (%)	2.86 ± 1.31	3.00 ± 0.96	0.548
DNA fragmented spermatozoa (%)	3.51 ± 2.23	3.61 ± 2.20	0.826
Alive spermatozoa (%)	52.60 ± 7.06	59.27 ± 8.61	0.028*
Western blotting (pixel)	2.47 ± 0.72	3.36 ± 3.23	0.283

All parameters except WB that were used for the analysis are the percentage of flow cytometric Annexin V assay results as necrotic, early necrotic, viable, apoptotic spermatozoa, and the ratio of DNA fragmented spermatozoa determined by TUNEL, the percentage of alive spermatozoa according to eosin-nigrosin test, the intensities () of BAX protein bands were calculated by the Image lab software following WB. All responses are compared between two groups and listed as mean and standard division including P-values.

Table 2.3 Pearson correlation coefficients with p-values

Variables	Correlation coefficient	p- value
Fertility score vs. Necrotic sperm (%)	-0.266	p=0.0113
Fertility score vs. Early Necrotic sperm (%)	-0.01	p> 0.05
Fertility score vs. Viable sperm (%)	0.072	p> 0.05
Fertility score vs. Apoptotic Sperm (%)	-0.063	p> 0.05
Fertility score vs. DNA Fragmentation (%)	-0.017	p> 0.05
Fertility score vs. Alive sperm (%)	-0.49	p=0.0056
Fertility score vs. Expressed BAX (pixel)	-0.301	p> 0.05
Necrotic spermatozoa (%) vs. Early Necrotic sperm (%)	-0.506	p<0.0001
Necrotic spermatozoa (%) vs. Viable sperm (%)	0.42	p<0.0001
Necrotic spermatozoa (%) vs. Apoptotic Sperm (%)	-0.688	p<0.0001
Necrotic spermatozoa (%) vs. DNA Fragmentation (%)	0.025	p> 0.05
Necrotic spermatozoa (%) vs. Alive sperm (%)	0.377	p=0.04
Necrotic spermatozoa (%) vs. Expressed BAX (pixel)	0.223	p> 0.05
Early Necrotic spermatozoa (%) vs. Viable sperm (%)	-0.991	p<0.0001
Early Necrotic spermatozoa (%) vs. Apoptotic Sperm (%)	0.358	p=0.0006
Early Necrotic spermatozoa (%) vs. DNA Fragmentation (%)	-0.039	p> 0.05
Early Necrotic spermatozoa (%) vs. Alive sperm (%)	-0.435	p=0.016
Early Necrotic spermatozoa (%) vs. Expressed BAX (pixel)	0.05	p> 0.05
Viable spermatozoa (%) vs. Apoptotic Sperm (%)	-0.367	p=0.0004
Viable spermatozoa (%) vs. DNA Fragmentation (%)	0.052	p> 0.05
Viable spermatozoa (%) vs. Alive sperm (%)	0.386	p=0.035
Viable spermatozoa (%) vs. Expressed BAX (pixel)	-0.094	p> 0.05
Apoptotic Spermatozoa (%) vs. DNA Fragmentation (%)	-0.126	p> 0.05
Apoptotic Spermatozoa (%) vs. Alive sperm (%)	-0.084	p> 0.05
Apoptotic Spermatozoa (%) vs. Expressed BAX (pixel)	-0.0832	p> 0.05
DNA Fragmentation (%) vs. Alive sperm (%)	-0.144	p> 0.05
DNA Fragmentation (%) vs. Expressed BAX (pixel)	-0.219	p> 0.05
Alive spermatozoa (%) vs. Expressed BAX (pixel)	0.23	p> 0.05



© 2000-2011 Ingenuity Systems, Inc. All rights reserved.

Figure 2.1 Apoptosis signaling pathway

The intrinsic and extrinsic pathways with the molecules that are involved in these pathways are represented. Molecular mechanisms of BAX and BCL-2 including their interaction with the mitochondria can also be seen. The picture was generated by IPA Pathway Analysis software.

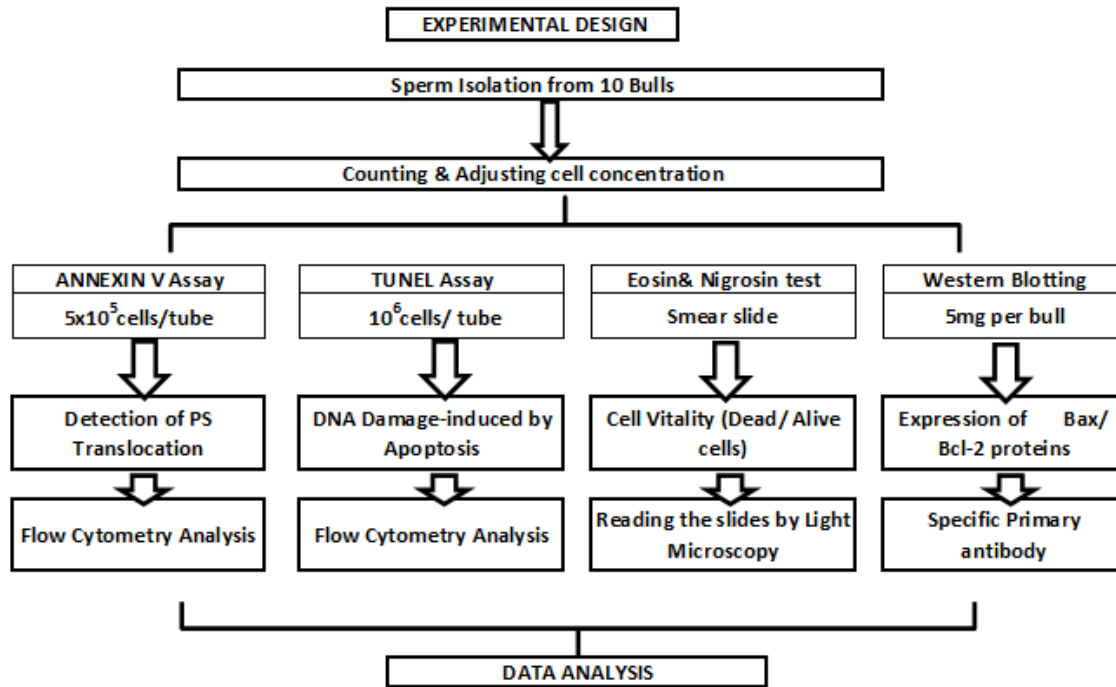


Figure 2.2 Experimental design

Overall, sperm samples from 10 bulls were used for each experiment. First spermatozoa were isolated and separated into four aliquots to perform each assay followed by counting. A total of nine reads per bull with three technical replicates in three different times was performed for TUNEL and ANNEXIN V experiments. Two technical replicates repeated three times results in six reads per bull were accomplished for eosin & nigrosin test, with a hundred spermatozoa counted per slide. Western blotting with three replicates was done using 5 µg of protein per bull for accuracy, and the intensity of protein bands in the pictures were determined via Image Lab software (Bio-Rad).

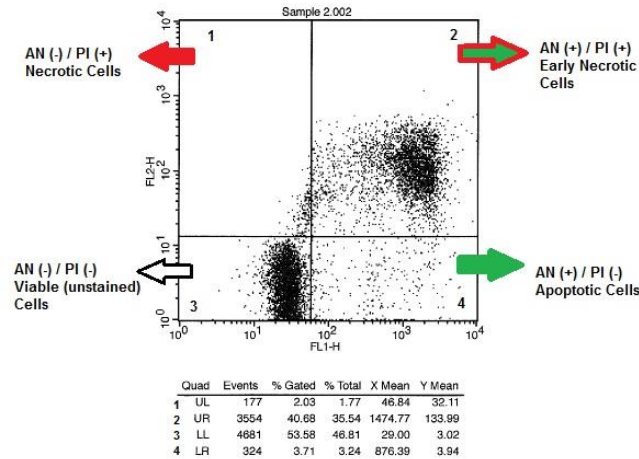


Figure 2.3 Sperm cell population by flow cytometry

Four distinct populations can be identified with AnnexinV/PI assay. While late necrotic spermatozoa were stained with PI, but not with Annexin V (UL), early necrotic spermatozoa were labeled with both Annexin V and PI (UR). Viable spermatozoa were stained with neither Annexin V nor PI (LL), while apoptotic spermatozoa were labeled with only Annexin V, but not with PI (LR).

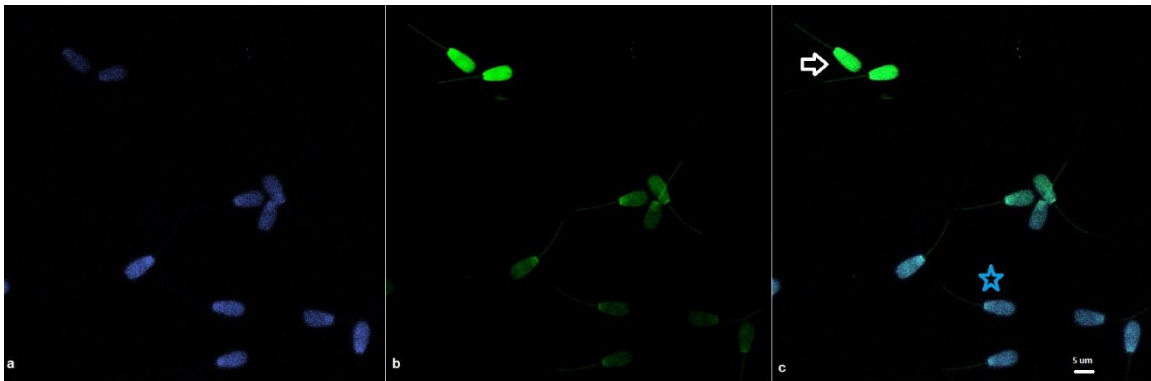


Figure 2.4 DNA Fragmentation detected by TUNEL assay using fluorescence microscopy

A: DAPI stained sperm samples with the DAPI filter. B: TUNEL assay with the FITC filter. C: Overlay of two images; white arrow indicates DNA fragmented sperm cells (apoptotic) which stained as green whereas blue star shows DNA integrity of the sperm (non-apoptotic) containing blue color.

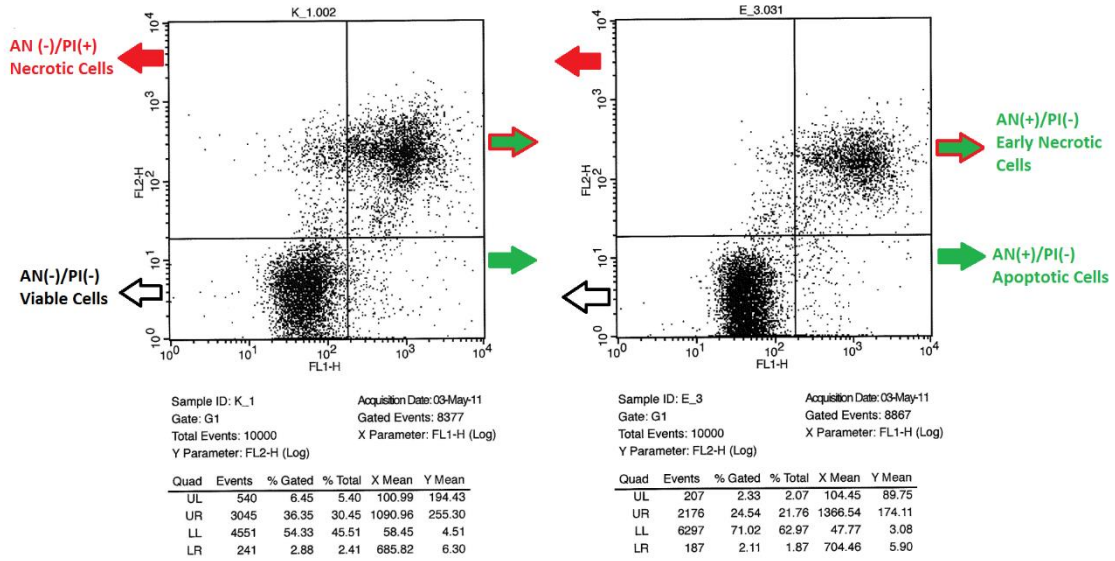


Figure 2.5 Sperm apoptotic cell population of two bulls with varying fertility by flow cytometry

K_1.002 (Bull 1) is a low fertility bull and E_3.031 (Bull 10) is a high fertility bull. The percentage of necrotic, early necrotic, viable and apoptotic spermatozoa gated can be seen in the tables and both can be seen in the figures and in the tables as UL (upper-left), UR (upper-right), LL (lower-left) and LR (lower-right), respectively.

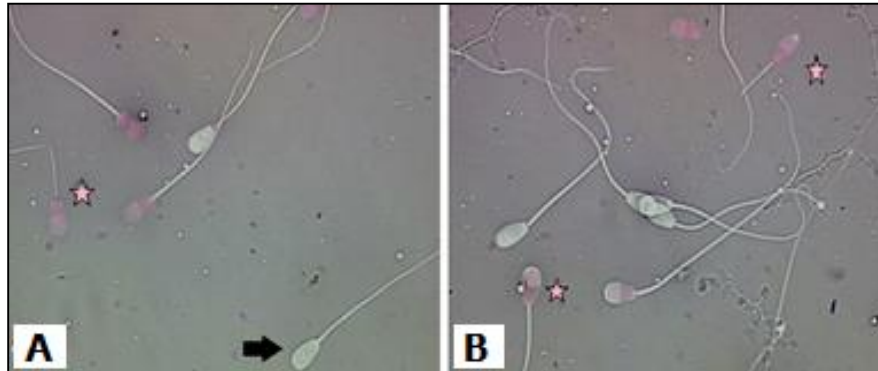


Figure 2.6 Eosin/nigrosin staining

Two microscopic slides of eosin-nigrosin stain from two different bulls are shown; live spermatozoa were not stained and are shown with a black arrow while dead spermatozoa were labeled with the stain marking with the star.

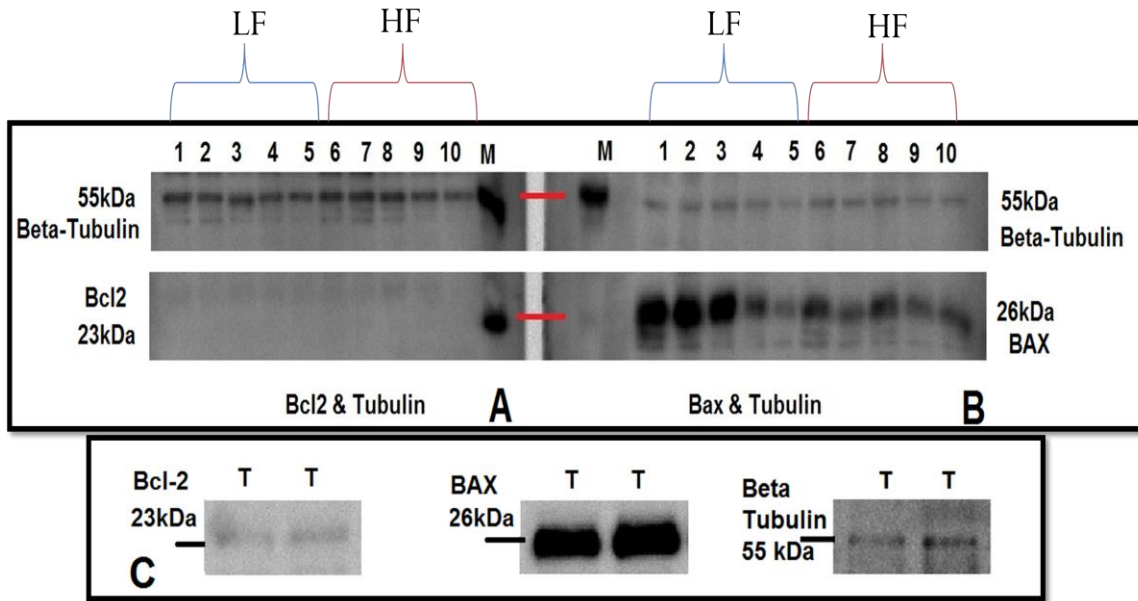


Figure 2.7 BAX, BCL-2 and Beta-Tubulin proteins

A: The expression of BCL-2 (anti-apoptotic) and β -Tubulin, B: BAX (pro-apoptotic) and β -Tubulin proteins among the bulls. C: The expression of BCL-2 and BAX proteins using the same testis sample as positive control. M: Marker, T: Testis. Ten bulls were presented with their numbers from low fertility to high fertility bulls 1 to 10, respectively. LF: Low Fertility, HF: High Fertility.

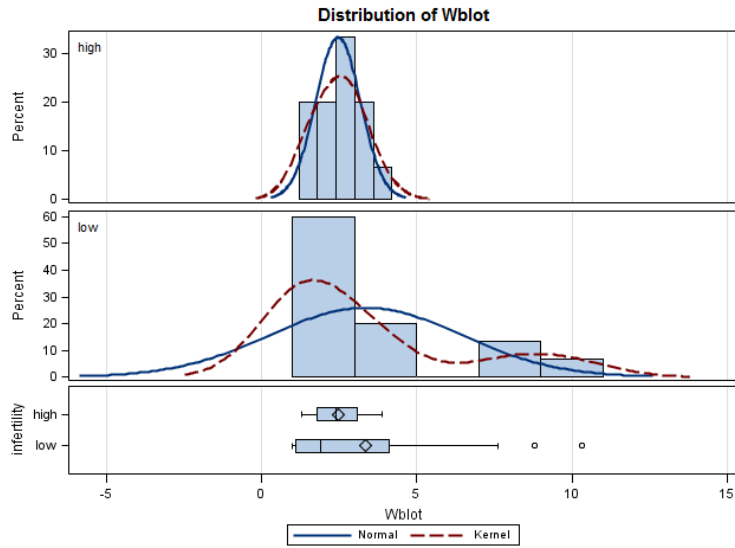


Figure 2.8 The distribution graph of Western Blotting data.

The distribution of western blotting data among the high vs. low fertility groups generated by SAS software are represented here. Each group contains five bulls and each bar in the graphs indicates a bull. The protein levels of each bull were calculated by the software (see material methods for details).

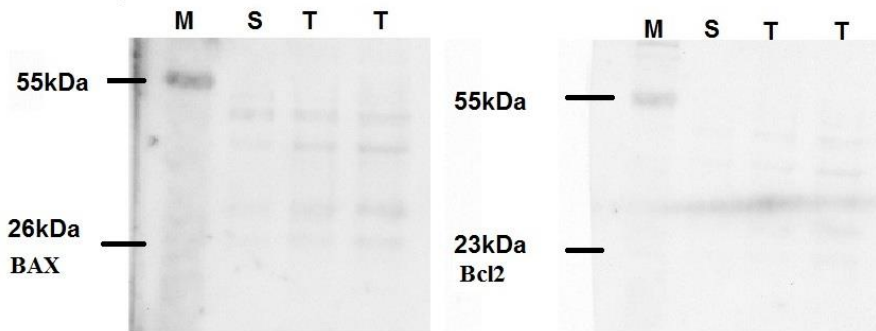


Figure 2.9 Western Blotting negative controls.

The negative control of western blotting experiments for both antibodies (BAX and BCL-2) where the only secondary antibodies [Donkey anti-rabbit IgG-HRP] were used. M: Marker, T: Testis, S: Sperm.

CHAPTER III

DYNAMICS OF SPERM CHROMATIN ASSOCIATED WITH FERTILITY

Abstract

Sperm provides the essential constituents playing vital roles in fertilization, early embryonic development and beyond. However, the nature and mechanisms of how sperm chromatin structure regulates fertility are not clearly defined. We aimed to determine expression dynamics of Protamine 1 (PRM1) and chromatin structure in sperm from bulls with distinct scores of fertility. While chromatin integrity and protamination were detected using the halomax assay and toluidine blue staining, the expression of PRM1 was identified by western blotting (WB), flow cytometry (FC), and immunocytochemistry (ICC). All of the experiments were repeated at least three times, and statistical analysis was performed using SAS. Defective chromatin condensation and protamination errors were significantly increased in sperm from low fertility bulls ($P < .0001$), while the expression of PRM1 was significantly abundant in high fertility bulls ($P = 0.0145$). Likewise, *in vivo* fertility scores of the bulls were found to be negatively correlated with protamination errors ($r = -0.62$; $P < .0001$) and defective chromatin condensation ($r = -0.69$; $P < .0001$) and that was positively correlated with PRM1 expression by WB ($r = 0.25423$; $P = 0.0500$) and by FC ($r = 0.61776$; $P = 0.0037$). Abnormal sperm showed a scattered localization of PRM1 in the pre-equatorial and acrosomal regions of their nuclei. These data suggest that lack of PRM1 might cause

inadequate chromatin protamination and fragmentation, leading to inefficient sperm chromatin condensation and consequently improper fertilization. These findings are significant to identify paternal influence on early development and to evaluate sperm viability across mammals using molecular phenotypes.

Introduction

Mammalian spermatozoon has amazingly small cytoplasm in which it contains condensed chromatin, whose DNA binding proteins are different than those in somatic cells. Packaging of sperm DNA is achieved by a doughnut (donut) model or torus containing highly basic arginine and cysteine rich protamines (PRM) in spermatogenesis [92]. During sperm chromatin remodeling, core (canonical) somatic histones are first replaced by their testis specific variants [21], and then by transition protein 1 (TP1) and transition protein (TP2) in the differentiating spermatids and subsequently by protamines. Unlike histones, protamines are different among species; for example, protamine 1 (PRM1) is found in mature spermatozoa of all mammals while protamine 2 (PRM2) packs sperm chromatin in primates, many rodents and other placental mammals [93]. Following fertilization, maternal histones will replace these protamines by taking advantage of some chaperone proteins such as histone chaperone protein, HIRA, and especially maternal histone variants [94]. Therefore, any defects to sperm chromatin occurring during spermatogenesis might affect downstream function of spermatozoa [17, 92]. The DNA regions packed by histones contain essential genes that are preferentially activated prior to fertilization compared to those that are bound to protamines. Recently, repressive and active histone methylation were identified to be epigenetic marks in human and mouse spermatozoa [95] with a regulatory function on transcription

machinery [64, 96] and on paternal epigenetic control during early embryonic development (reviewed by [97]).

In addition to apoptosis and oxidative stress, defective chromatin packaging in spermatozoa is one of the underlying reasons for damage of DNA, which ultimately causes male infertility [48]. Sperm chromatin alterations were demonstrated to be critical in fertilization and early embryonic development. Therefore, several clinical techniques have been used to detect defective chromatin condensation in spermatozoa including the sperm chromatin structure assay (SCSA), TUNEL assay, single-cell gel electrophoresis (SCGE: COMET) assay, the sperm chromatin dispersion (SCD) test, DNA breakage detection- fluorescent in situ hybridization (DBD-FISH), toluidine blue (TB) and aniline blue staining (reviewed by [35]). One of the common techniques is the SCD test that relies on the degradation of sperm chromatin via proteolysis [98]. It is commercially modified to be used for diagnostic purposes in both animals as Halomax® [42, 99-105] and in humans as Halosperm® [100, 106-108]. In addition to DNA damage in sperm, other groups have demonstrated the expression patterns of *prm1* transcripts in males [109], including protamine-deficient animal models [110]. The evaluation of protein ratios such as Protamines [25, 29, 64, 65] and/or histone/protamine [66] were also illustrated to diagnose male infertility. Later on, studies detected the specific DNA regions targeted by protamines and/or histones in human sperm [96] and identified particular epigenetic modifications; such as histone acetylation and methylation of the *prm1* gene domains in mouse spermatogenesis [111]. This led to the demonstration of *in vivo* phosphorylation of protamines during spermatogenesis [112] as well as *in vitro* phosphorylation of P2 in mammalian sperm, excluding bull and ram sperm [113].

In contrast to compensatory fertility that can be improved by increasing the amount of spermatozoa, non-compensatory fertility is considered to be due to molecular defects in sperm resulting in sub-par fertility [47]. We now know that male infertility may be either directly or indirectly related to the ratio of histone-retention as well as protamine-condensation in spermatozoa, but what we do not know is to what extent sperm DNA compaction influences male fertility. Therefore, the objectives of this study were to determine the expression patterns of Protamine 1 and to examine chromatin integrity in spermatozoa from bulls with varying fertility, including the role of Protamine 1 in early embryonic development. By having only PRM1, bull sperm will serve as a model to provide further knowledge about the functions and interactions of the chromatin remodeling factors in sperm physiology as well as male fertility. This study is the first detailed PRM1 profiling of spermatozoa from bulls with distinct phenotypic data, providing a practical knowledge on the nature and function(s) of PRM1 in sperm. Hence, such information will be used not only to improve bull fertility in the field, but will also be incorporated into human studies as well.

Material and Methods

Cryopreserved semen samples from bulls with distinct fertility were obtained from Alta Genetics, Inc. (Watertown, WI, USA). Unless otherwise indicated, all chemicals were purchased from Sigma-Aldrich Chemicals (St. Louis, MO, USA).

Determination of bull fertility

Bull fertility scores were determined using Probit F90 software [75] and have been used in the Alta Advantage Program (Alta Genetics Inc., WI, USA). This program is

periodically updated by updating bull fertility information from partnering dairy producers [72]. In this program, environmental factors and herd management have been optimized using reliable threshold models [73], [74]. For this study, we used the SD of the population as the criterion to classify bulls as high and low fertility. The details of selection criteria were explained in the related section of chapter II.

Isolation of spermatozoa

Straws of semen from twenty bulls (Table 3.1) were thawed in a 37°C water bath for 1 min, and then spermatozoa were washed with warmed PBS (Gibco, CA, USA) and centrifuged twice at 700g for 15 min and 10 min. The sperm pellets were then re-suspended in warmed PBS and cell concentration was adjusted to 25 to 30x10⁶ cells / mL using a hemacytometer. Spermatozoa were incubated at 37°C prior to the toluidine blue and halomax experiments for accuracy. For western blotting (WB), the sperm pellets were stored at -80°C until extraction of protein.

Chromatin maturity and integrity approaches

Toluidine blue (TB) cytometry

The TB dye is a sensitive external agent which can incorporate itself into the damaged dense chromatin; at which time, it becomes metachromatic upon binding. In this study, the TB staining was used to determine the maturity of sperm chromatin and DNA integrity as earlier described [114]. Briefly, smear slides were prepared by putting one sperm drop of 50 µL on a microscope slide and then using a back edge of an angled cover slip to spread the drop over the slide leading to approximately 1x 10⁶ spermatozoa per slide. For fixation, slides were soaked in ethanol acetic acid (3:1, V/V) for 1 min and then

immersed in 70% ethanol for 3 min following hydrolyzation. Slides were then air dried after washing with distilled water. Staining was performed using 200 μ L of 0.025% TB in McIlvaine buffer (sodium citrate-phosphate; pH4.0). Then, 500 spermatozoa /slide were evaluated using a light microscope with 100 x objectives. Spermatozoa stained from green to light blue were considered to have normal chromatin while the ones stained from dark blue to violet were considered to have abnormal chromatin (Figure 3.1).

Sperm Chromatin Dispersion Test (SCD)/Halomax

Halomax kit was used to determine DNA fragmentation in spermatozoa according to the company's instructions (Halotech DNA SL, Spain). Briefly, a 1.5- 2 μ L drop of the cell suspension was adjusted to 10 to 20x10⁶/mL and embedded into 50 μ L of melted agarose supplied with the kit and covered with a 24x24mm cover slip. The slides were processed with the lysing solution supplied with the kit at room temperature (22°C) and with distilled water. Following dehydration, slides were air dried and stored at room temperature prior to Wright-Giemsa (Wright solution, Fisher Scientific, Pittsburg, PA, USA) staining. Five hundred cells per slide were evaluated by a light microscopy with a 60x objective, and spermatozoa with a small and compact halo of chromatin dispersion were considered non-fragmented DNA in contrast to spermatozoa with a large and spotty halo of chromatin dispersion (Figure 3.2).

Expression of the PRM1 Approaches

Sperm nuclear protein isolation

Cryopreserved spermatozoa from 20 bulls (10 high vs.10 low fertility bulls) were thawed and washed three times using PBS supplemented with phenylmethylsulfonyl

fluoride (PMSF). Extraction of nuclear proteins were performed using an acetic acid-urea (AAU) system according to a previous study[115]. Briefly, following centrifugation, sperm pellets were re-suspended in 100 μ L of 20 mM EDTA, 1mM PMSF, 100 mM Tris (pH8.0), and then 100 μ L of 6M guanidine Hydrochloride (HCl) and 575 mM DTT were added into this suspension. After the addition of 1mL of ethanol, each sample was then incubated at -20°C for 1 min and then centrifuged twice for 15 min. Subsequently, 1mL of 0.5M HCl was added to the sperm pellets, which were then incubated at 37°C for 15 min. Following centrifugation at room temperature for 10 min, 300 μ L of TCA at 4°C was added to the supernatant, which was then centrifuged at 4°C for 10 min. Afterwards, sperm pellets were washed with 500 uL of 1% 2-mercaptoethanol in acetone, followed by air-dry. The cell lysates were re-suspended in 50 μ L of 5.5 M urea, 20% 2-mercaptoethanol and 5% acetic acid. The supernatant containing the proteins were then diluted by ddH₂O [1/20.000 or 1/30.000] and quantified using microBCA protein assay (Thermo Scientific Inc., Rockford, IL, USA) method according to the manufacturer's recommendations. Following incubation, protein quantifications were detected via spectrophotometer and calculated using the software SoftMax Pro5.2 Rev C (Molecular Devices, Sunnyvale, CA, USA). We used testis extract (T), fibroblast extract (F), and a sperm sample with unknown fertility as positive, negative and random controls, respectively (Figure 3.3a). The concentration vs. mean OD values was also calculated and displayed with a linear fit [one of which was shown as an example here: $y=A + Bx$, while A; 0.0336 and B; 0.0169 and R²; 0.999 as a plot (Figure 3.3b)]. Protein samples were then stored at -80°C until WB experiments.

Immunodetection of nuclear proteins using WB

Equal amounts of the isolated proteins were separated in acetic-acid-urea gel (Table 3.2) system according to a previous study [115] , and then transferred onto polyvinylidene fluoride (PVDF) membranes using the semi-dry transfer method with HEP-1 Semidry Electroblothing (Thermo Scientific Inc. Rockford, IL, USA). The membrane was then blocked with 1xTris buffered saline with 1% casein at room temperature for 60 min (Bio-Rad, CA, USA) and then incubated with the primary antibody against Protamine1 (sc-23107, Santa Cruz, CA, USA) at 4°C overnight. The membrane was then washed three times at room temperature for 15 min each with washing buffer containing 0.1% Tween20, followed by incubation with secondary antibodies conjugated to horseradish peroxidase (Donkey anti-goat IgG-HRP, sc-2033 from Santa Cruz, CA, USA) at room temperature for 60 min. Subsequently, chemiluminescent substrate (WBKLS0500, Millipore MA, USA) was added to the membrane to detect the signals. The intensities of the bands were quantified using Image Lab software (Bio-Rad, Hercules, CA, USA). Bovine fibroblast cells were utilized as a negative control while testis lysate (See the related protocol in Appendix) was used as a positive control for this specific antibody. Following immunoblotting, the intensities of protein bands were analyzed and quantified using Image Lab software (Bio-Rad). We also confirmed the protein expressions using a different primary antibody, PRM1 (Hup-1N-150, Briar Patch Biosciences LLC, CA, USA) and a secondary antibody, (Donkey anti-rabbit IgG-HRP, sc-231, Santa Cruz, CA, USA) (data not shown).

Immunocytochemistry and flow cytometry

Flow cytometry

Following permeabilization with the 0.15 % stock solution of Triton X-100 (final concentration: 0.1%), samples were -incubated for 40 minutes at room temperature. For flow cytometry, 100 μ L of sperm suspension containing $2-50 \times 10^5$ spermatozoa /mL were labeled in a 96-well plate (Becton Dickinson Labware, Franklin Lakes, NJ, USA; catalog #353915). After overnight incubation of the primary antibody (PRM1 #cat No: 1/50) at 4 °C, the goat anti-rabbit secondary antibody conjugated to green dye FITC (Zymed Laboratories, San Francisco, CA, USA) was used at a final 1:200 dilution in PBS + 0.1% Triton X-100 . Fluorescent labeling of the samples were tested using the epifluorescence microscope Nikon Eclipse 800-microscope (Nikon Instruments Inc., Melville, NY, USA) prior to the flow cytometry. The approximate concentration of sperm suspensions was adjusted to be 5×10^5 spermatozoa per well and positive labeling was also confirmed. Sperm flow cytometer EasyCyte Plus 142 (IMV Technologies, L'Aigle, France) was utilized for flow cytometric analysis [116]. According to data analysis measured by the flow cytometry, a histogram and a scatter diagram for each sample were also recorded. A standardized histogram was also produced by measuring the fluorescence of specific sperm populations. According to this output, three specific sperm populations were labeled with Alexa 156 Fluor 488-conjugated secondary antibody. The first area was represented by a limited/absent fluorescence peak of the specific protein (PRM1), which was named M1. The second peak indicated with M2 represented a normal fluorescence intensity of the specific protein while the M3 peak contained abnormal fluorescence intensity. The scatter diagrams consisted of the

percentage of the spermatozoa within the aforementioned areas (M1, M2 and M3) and the relative fluorescence intensities based on these histograms.

Immunocytochemistry (ICC) and Cell Imaging

Immunocytochemistry was performed according to the protocol previously published [117]. As previously described, the ubiquitine (UBB) protein was also used as a negative marker of sperm fertility in this study as well [118]. For ICC experiments, 20 μ L of spermatozoa were fixed and then were mounted on lysine-coated microscopy coverslips, followed by permeabilization with 0.1% Triton TX-100 (Sigma-Aldrich, St. Louis, MO, USA). By selecting the specific primary antibody for PRM1 in spermatozoa, the spermatozoa were blocked with 5% normal goat serum for 25 min. After blocking, the samples were incubated with rabbit polyclonal PRM1 primary antibody for 40 min. The mouse polyclonal Ubiquitine MK12-3 primary antibody was also used for a double-labeling. Subsequently, the coverslips were incubated with a mixture of the secondary antibodies containing the goat anti-rabbit IgG-FITC for PRM1, the goat anti-mouse IgG-92 TRITC for ubiquitine and the DAPI staining for DNA for 30 min. For the negative control, only the secondary antibody was used without the primary antibody. For the negative control, NRS for 1/200 GAM-FITC primary antibody was used while the positive control contained DNase treatment without DAPI staining (Figure 3.10b and c, respectively). Afterwards, spermatozoa were evaluated using the Nikon Eclipse 800-microscope (Nikon Instruments Inc., Melville, NY, USA), including the Cool Snap CCD camera (Princeton Instruments Trenton, NJ, 100 USA) and MetaMorph software (Molecular Devices Inc., Sunnyvale, CA, USA). Following examination of the slides,

images were processed and edited by Adobe Photoshop CS3 Extended software (Adobe Systems Inc., San Jose, CA, USA).

Statistical analysis

The percentage data obtained from the expression of PRM1 by WB, the ratio of chromatin condensation by halomax, and the percentage of protamination by TB staining was first verified to be normally distributed by the Shapiro-Wilk test and Kolmogorov-Smirnov (K-S) test using PROC UNIVARIATE command in SAS Version 9.2 for Windows (SAS Institute, Cary, NC, USA). Total numbers of measurements were then classified into two groups, high and low fertility bulls, and then analyzed using one way ANOVA test with PROC ANOVA command in SAS, including mean values (\pm SD). Since we designed the experiments based on the 3 \times 2, 3 \times 2 and 3 replicates per bull for the chromatin condensation and protamination and WB, respectively, we analyzed the data using the ANOVA test. Overall relation among the data was performed using Pearson correlation analysis with PROC COR command in SAS, determining any significant ($\alpha \leq 0.05$) linear associations between fertility, chromatin condensation, protamination and expression of PRM1; regardless of any grouping. Following a stepwise multiple regression analysis using PROC GLMSELECT command in SAS, the regression analysis of the selected variables was performed by PROC REG to determine which combination of measured variables might best predict fertility.

Results

Distinct fertility differences exist among the bulls

Having the most reliable fertility data from more than 1,000 bulls analyzed by Probit F90 software, fertility of high vs. low fertility groups were $4.56 \pm 0.77\%$ vs. $-7.44 \pm 3.3\%$ of the average, called 0, respectively. The average of insemination was for the high and low fertility groups were $754.9 \pm 345.0\%$ vs. $782.7 \pm 282.9\%$, respectively (Table 3.3).

Extent of proper protamination differs in sperm from high vs. low fertility bulls

Because TB can distinguish the maturity of spermatozoa by binding to histones instead of protamines, it was used to determine the extent of proper protamination in bull spermatozoa. Toluidine blue staining in spermatozoa was displayed in Figure 3.1. In this figure, spermatozoa with protamination errors were stained as purple-dark blue and indicated with a star whereas normal protamination was displayed with light blue. The ratio of spermatozoa containing alterations in DNA condensation was $1.9\% \pm 0.97$ vs. $3.27\% \pm 0.99$ for high vs. low fertility bulls, respectively ($P < .0001$; Figure 3.4a and Table 3.3). Furthermore, *in vivo* fertility scores of the bulls were negatively correlated with improper chromatin protamination ($r = -0.62$; $P < .0001$). Likewise, protamination errors was negatively correlated with the expression of PRM1 in spermatozoa ($r = -0.30190$; $P = 0.0191$; Table 3.4). Results of the TB experiments performed by two technicians were the same $2.57 \pm 1.11\%$ vs. $2.62 \pm 1.23\%$ ($P > 0.80$).

Fragmentation status of sperm chromatin is different in high vs. low fertility bulls

The defective chromatin condensation associated with histone-protamine transition errors were detected as DNA fragmentation using a commercially available sperm chromatin dispersion (SCD) test, Halomax. Our results showed a distinct difference in sperm from high ($4.13\% \pm 0.84$) vs. low ($7.01\% \pm 2.24$) ($P < 0.0001$) fertility bulls (Figure 3.4b and Table 3.3). Sperm DNA fragmentation was negatively correlated with *in vivo* fertility scores of the bulls ($r = -0.69$; $P < 0.0001$). There was also positive correlation between protamination errors and defective chromatin condensation in spermatozoa ($r = 0.50515$; $P < 0.0001$). However, defective chromatin condensation were not correlated with the expression levels of PRM1 ($r = 0.10321$; $P > .05$) (Table 3.4). Using the Halomax assay, DNA fragmentation detected in spermatozoa was represented in Figure 3.2. In this figure, spermatozoa with defective chromatin condensation were dispersed as fragmented and indicated with arrows, whereas non-fragmented spermatozoa had intact nuclei. Results obtained by two technicians for this assay were the same $5.6 \pm 2.32\%$ vs. $5.36 \pm 2.28\%$ ($P > 0.54$) (Table 3.5).

Expression of PRM1 by immunoblotting is diverse in sperm from high vs. low fertility bulls

Using the acetic-acid-urea (AAU) gel system, sperm nuclear proteins from different bulls were run and then stained using Coomassie Blue staining (Figure 3.5). This gel system allowed us to distinguish the molecular weights of PRM1 (5 kDa) from those of histones (> 14 kDa). The intensities of two bands from bovine fibroblast cells (as negative control) and spermatozoa were evaluated (Figure 3.6a and 3.6b, respectively). Following immunoblotting with the specific primary antibody, the PRM1 intensities of

bands in spermatozoa were determined to be 6.15 ± 3.6 and 3.96 ± 3.09 in high vs. low fertility bulls, respectively ($P=0.0145$) (Figure 3.4c and Table 3.3). The signal intensities of the expressed proteins were first determined by Image Lab software (Bio-Rad, Hercules, CA, USA) and then they were normalized to the weakest band in the gel, which was bull #9. Expression of PRM1 was negatively correlated with *in vivo* fertility scores of the bulls ($r=0.25423$; $P=0.0500$; Table 3.4). According to immunoblotting results, PRM1 profiling of sperm from 20 bulls with varying fertility was shown in Figure 3.7. While bovine fibroblasts were used as a negative control, bull testis lysate was used as a positive control (See the related protocols in Appendix).

In this study, the predictive regression for fertility from the two parameters (< 0.05) was detected using stepwise regression analysis and calculated as fertility = $12.07 - 2.35TB - 1.32Halo$. According to the stepwise multiple regression analysis with fertility as a dependent variable, two predictors were; the TB value indicating the percentage of protamination errors and the Halo value containing the percentage of defective chromatin condensation.

Flow cytometric analysis of PRM1 expression in sperm from high and low fertility bulls

According to our flow cytometric measurements of PRM1, three fluorescence areas containing M1, M2 and M3 plots were detected in spermatozoa from high vs. low fertility bulls and were displayed in a histogram (See Figure 3.8a and 3.8b, respectively). The percentage of M1 was negatively correlated with *in vivo* fertility scores of the bulls ($r=-0.56433$; $P=0.009540$) (Figure 3.9a). There was a positive correlation between the Protamine M1 median fluorescence and fertility scores ($R=0.66033$; $p=0.00153$; Figure

3.9b). The median of protamine total fluorescence was a positively correlated with 20 bulls with higher fertility ($r= 0.5909$; $P= 0.00608$; Figure 3.9c), whereas the rate of M2 revealed a positive correlation with the aforementioned parameter ($r=0.61776$; $P=0.0037$; Figure 3.9d). On the other hand, there were no correlations between the percentage of M3, protamine M2 median, and protamine M3 median fluorescence with *in vivo* fertility scores of the bulls (%M3: $r=-0.3529$; $P=0.12696$), M2: $R=0.32543$; $p=0.16148$, M3: $r=-0.3529$; $P=0.12696$; Table 3.4)

Localization of PRM1 is varying in sperm from high and low fertility bulls

Cellular localization of PRM1 in normal and defective spermatozoa was detected using ICC and displayed in Figure 3.10a-o. According to ICC results, PRM1 was mostly localized in the equatorial and post-equatorial regions of nucleus in sperm with normal morphology (Figure 3.10a), while abnormal sperm showed a scattered localization of PRM1 in the pre-equatorial and acrosomal regions of their nuclei (Figure 3.10d-o). Positive and negative labeling of ICC is also represented in Figure 3.10b and 3.10c, respectively.

Discussion

Sperm DNA condensation takes place during spermatogenesis, which becomes de-condensed again in fertilization. Protamines are one of the main factors playing a role in the DNA condensation and re-condensation processes in mammalian sperm. A lack of protamination is considered a chromatin alteration and leads to abnormal maturation of sperm, causing sperm dysfunction and ultimately male infertility. Therefore, immature spermatozoa contain more histone-packaged chromatin regions in their genome and tend

to be more susceptible to DNA damages than mature spermatozoa that are packed mostly by protamines. Severity of DNA damage and chromatin packaging anomalies in spermatozoa were also demonstrated as origin of sperm dysfunction in sub-fertile men [29]. However, dynamics of sperm chromatin and impacts of paternal fertility in early embryonic development are not fully known. Hence, the objectives of this study were to determine the expression patterns of PRM1 and to examine chromatin integrity in spermatozoa from bulls with varying fertility, including the role of PRM1 in early embryonic development.

Sperm chromatin integrity was previously evaluated using simple staining assays such as TB and aniline blue [114]. According to our results, TB was sufficient to detect protamination among bulls. The protamination was significantly decreased in low fertility bulls compared to their highly fertile counterparts. The first study in which Halomax was used in bull sperm established a relationship between fertility and sperm chromatin fragmentation via light bright microscopy and fluorescence microscopy. Although there was no correlation between results of the SCSA and the Halomax test, the percentage of fragmented DNA detected via bright light microscopy was established to be one of four parameters predicting fertility of sperm samples in the same study [42]. We also showed in our study that spermatozoa with fragmented DNA using the Halomax kit were detectable via light microscopy. Halomax was found to be one of two parameters to estimate bull fertility in our study. Later on, it was demonstrated that measuring sperm DNA fragmentation (SDF) by Halomax might indicate a successful AI in the field with a critical value of 7 to 10% of fragmented spermatozoa in the semen [119]. Our results agreed with the findings of the previous study and we concluded that defective chromatin

condensation in spermatozoa was associated with male infertility. The Halomax test was concurrently used with the SCSA assay in bulls by another study establishing a positive association with the detection of sperm chromatin fragmentation, but not with the age of the bull. In addition, sperm chromatin fragmentation was correlated with sperm head abnormalities in the same study [101]. According to our ICC results, we demonstrated improper distribution of PRM1 in nuclei of abnormal spermatozoa compared to their morphologically normal counterparts. In addition to localization of PRM1, chromatin condensation was found to be related to the expression patterns of PRM1 in bull sperm.

We previously demonstrated that *prm1* transcript is highly expressed in bovine sperm from high fertility bulls compared to their low fertility counterparts, suggesting that *prm1* might be the one of the sperm ‘fingerprints’ [120]. In contrast to bull sperm, PRM1 and PRM2 equally pack DNA in mouse sperm whereas human sperm contains PRM1, 2 and 3 at the same time, leaving 15% of its chromatin packed with histones [29]. The majority of previous studies were carried out to determine a ratio of PRM1 and 2 in infertile men compared to their fertile counterparts [25, 29, 64, 65], whereas the remaining studies were focused on the relative amount of histone over protamines [66]. Males with ratios of increased histones to protamines tended to have an increased likelihood of infertility problems [121]. In addition to histone/protamine ratio, P1/P2 ratio in human spermatozoa is considered as prognostic criterion in infertile men [122-124] and in the development of human preimplantation embryos [125]. In the current study, we demonstrated that PRM1 was abundant in spermatozoa from high fertility bulls and that PRM1 was positively associated with male fertility in bulls. Therefore, we suggested that mature bull sperm chromatin is only packed with PRM1, which was established by

other groups [27, 28]. However, according to our multiple regression analysis, the expression patterns of PRM1 were not found to estimate fertility score in bull sperm. We suggested here that evaluating sperm chromatin integrity by detecting protamination status and fragmentation pattern might be sufficient to predict bull fertility in the field.

Using frozen sperm samples could be one of the limitations of the current study. However, our overall goal was to improve sperm chromatin integrity and ultimately, male fertility in the field and clinics. Our initial plan was to use histones along with the PRM1; however, by having different molecular weights, histones could not be included into WB. The reason for this was that the difference in molecular weight of histones (>14kDa) and PRM1 (5kDa) during transfer time and speed. We could not transfer these proteins in the same membrane at one time and currently. In addition to core histones, the detection of other histone variants with similar sizes (between 14-17 kDa) interfered with the specificity of the primary antibodies. Therefore, we only focused on PRM1 in the WB experiment, and included the Coomassie blue gel image to display the distribution of histones vs. PRM1 in AAU gel. We had a slight variation between WB trials; it might have been because of the challenges in the extraction of nuclear proteins and/ or the changes of sperm population from different straws/ collections per repeats.

In conclusion, our data showed that inadequate sperm chromatin protamination and integrity were associated with inefficient sperm chromatin condensation leading to improper fertilization and beyond, which can be estimated using bull fertility scores prior to use for AI. The current study is the first study identifying PRM1 expression in spermatozoa from bulls with varying fertility. We speculated that this unique expression

of PRM1 in bovine mature spermatozoa might be used as a model in studies on protamine transition during sperm chromatin condensation.

Acknowledgements

This study was funded in part by Mississippi Agricultural Forestry Experiment Station, The Conselho Nacional de Desenvolvimento Científico e Tecnológico, CNPq of Brazil, Alta Genetics, Inc, and Dr. Peter Sutovsky of the University of Missouri-Columbia.

Table 3.1 List of bulls and fertility data used for this study.

	NAAB#	Inseminations	Fertility
1	11HO8697	855	-14.7
2	11HO9832	595	-12.3
3	11HO7286	1552	-8.1
4	11HO9415	719	-7.2
5	11HO9692	668	-6.4
6	11HO9623	750	-6.3
7	11HO8529	781	-5.9
8	11HO9354	702	-5.6
9	11HO6975	783	-4.2
10	11HO9619	422	-3.7
Mean (±SD)		782.7 (± 282.9)	-7.44 (±3.3)
11	11HO8852	1024	3.3
12	11HO6893	1466	4
13	11HO8812	1039	4
14	11HO7130	651	4.2
15	11HO7332	578	4.5
16	11HO8020	904	4.8
17	11HO7751	300	4.8
18	11HO9402	518	4.8
19	11HO5985	326	5
20	11HO8869	743	6.2
Mean (±SD)		754.9 (±345.0)	4.56 (±0.7)

Total of twenty bulls (Low fertility: 1-10 and high fertility: 11-20) used for this study, the average insemination numbers and the fertility scores of these bulls, displayed as mean ± SD.

Table 3.2 Mean difference of parameters in high vs. low fertility bulls.

	Low Fertility Mean (\pmSD)	High Fertility Mean (\pmSD)	Total Mean (\pmSD)	N	Min	Max	p-value
Number of Inseminations	782.7 (\pm 282.9)	754.9 (\pm 345.0)	768.8 (\pm 314.5)	20	00.0	552	0.6302
Fertility Score	-7.44 (\pm 3.34)	4.4 (\pm 0.55)	-1.44 (\pm 6.5)	20	14.7	.2	<.0001
Protamination errors (%)	3.27 (\pm 0.99)	1.9 (\pm 0.97)	2.6 (\pm 1.2)	120	.8	.2	<.0001
Defective chromatin condensation (%)	7.01 (\pm 2.24)	4.13 (\pm 0.84)	5.6 (\pm 2.2)	120	.2	2.8	<.0001
PRM1 expression by WB	3.96 (\pm 3.09)	6.15 (\pm 3.6)	5.1 (\pm 3.5)	60	.0	2.9	0.0145

The mean differences of the data obtained from the expression of PRM1 by western blotting (WB), ratio of defective chromatin condensation by Halomax and the percentage of protamination errors by Toluidine blue (TB) staining in two groups and together are displayed as Mean \pm standard deviation (SD), Min and Max values, including p values.

Table 3.3 Pearson Correlation Coefficients

	Correlation Coefficients	P-value	N
<i>In vivo</i> Fertility Scores vs. Protamination errors (%)	-0.61757	<.0001	120
<i>In vivo</i> Fertility Scores vs. Defective chromatin condensation (%)	-0.68125	<.0001	120
<i>In vivo</i> Fertility Scores vs. PRM1 expression by Western Blotting	0.25423	0.0500	60
<i>In vivo</i> Fertility Scores vs. PRM1 total fluorescence by Flow Cytometry	0.5909	0.00608	20
<i>In vivo</i> Fertility Scores vs. PRM1 %M1 by Flow Cytometry	-0.56433	0.00954	20
<i>In vivo</i> Fertility Scores vs. PRM1 M1 median by Flow Cytometry	0.66033	0.00153	20
<i>In vivo</i> Fertility Scores vs. PRM1 %M2 by Flow Cytometry	0.61776	0.0037	20
<i>In vivo</i> Fertility Scores vs. PRM1 M2 median by Flow Cytometry	0.32543	0.16148	20
<i>In vivo</i> Fertility Scores vs. PRM1 M3 median by Flow Cytometry	-0.3529	0.12696	20
Protamination errors (%) vs. Defective chromatin condensation (%)	0.50515	(<.0001)	120
Protamination errors (%) vs. PRM1 expression	-0.30190	(0.0191)	120
Defective chromatin condensation (%) vs. PRM1 expression	0.10321	(0.4326)	120

In this figure, Pearson Correlation Coefficients (r) and their p values were represented using all data obtained from Protamine1 (PRM1) values by western blotting and flow cytometry, the ratio of chromatin maturity by Halomax, and the percentage of protamination by Toluidine blue staining regardless of grouping.

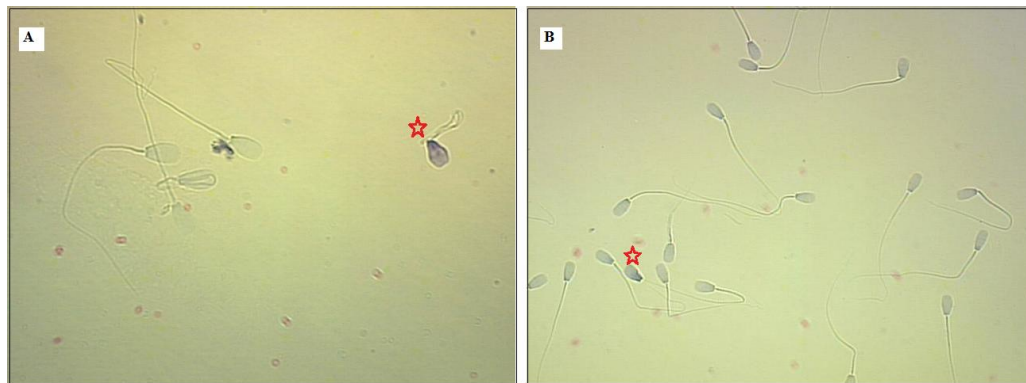


Figure 3.1 Toluidine Blue (TB) Staining Results

In this figure, TB dye that is a sensitive metachromatic external agent is being incorporated into the damaged dense chromatin following its binding is displayed in spermatozoa from different samples (A and B). Spermatozoa with protamination errors were stained as purple-dark blue and indicated with a star, whereas normal protamination was displayed with light blue.

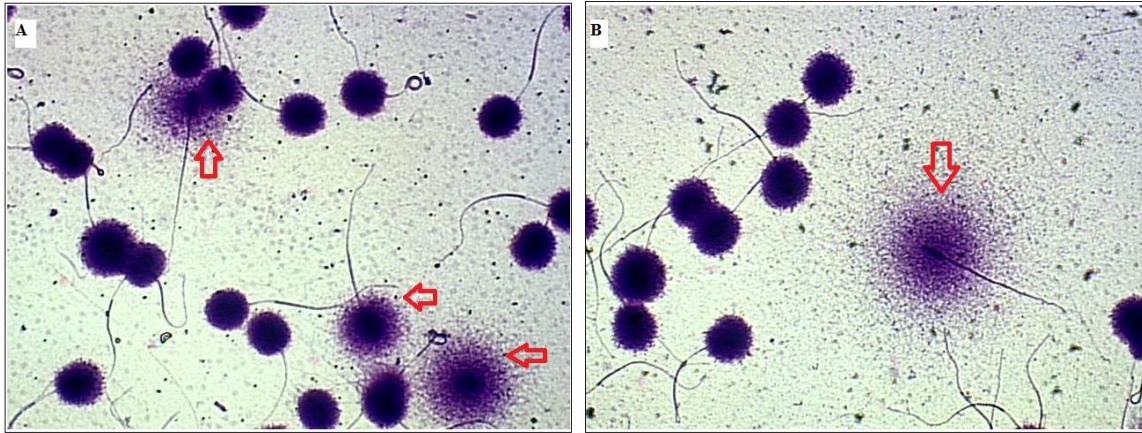


Figure 3.2 HaloMax® (Sperm Chromatin Dispersion) Test Results

Using the Halomax assay, DNA fragmentation detected in spermatozoa was represented in this figure. Spermatozoa with chromatin fragmentation were dispersed and indicated with arrows, whereas spermatozoa with non-fragmentation had intact nuclei.

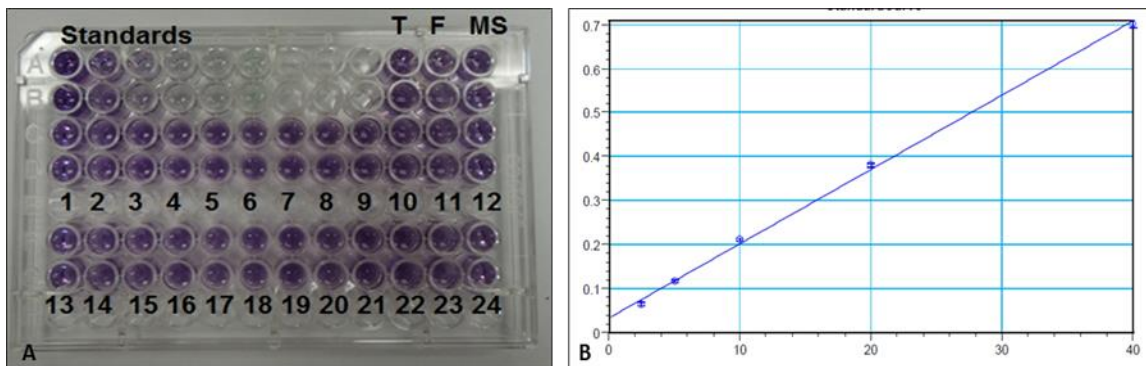


Figure 3.3 Protein quantification using micro BCA protein assay

Following incubation, protein quantifications were detected via a spectrophotometer and calculated using the software SoftMax Pro5.2 Rev C. A) A set up of a 96-well plate includes standards supplied with the kit, BSA (bovine serum albumin), Testis extract (T), fibroblast extract (F). MS: Sperm from Mississippi bull with unknown fertility score. 1-12: Low fertility bulls, 13-24: high fertility bulls. B) Standards; x-axis; Concentration vs. y-axis; Mean OD values, Linear fit: $y=A + Bx$, while A; 0.0336 and B; 0.0169 and R^2 ; 0.999

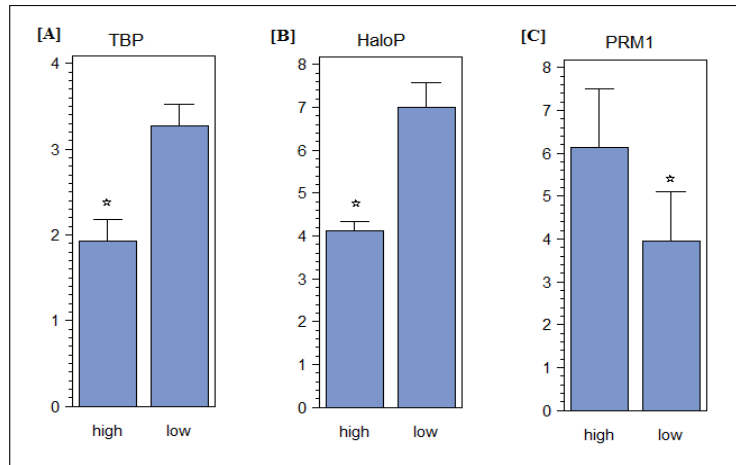


Figure 3.4 Distribution of chromatin integrity in sperm

The distribution graphs of data from Toluidine blue staining (TBP), Halomax test (HaloP), and the expression pattern of Protamine1 (PRM1) by Western Blotting (WB) in high vs. low fertility bulls are presented here in figure A, B and C, respectively. While the x-axis represents fertility groups, the y-axis is percentage values for TBP and HaloP and intensity of bands by pixel for PRM1. Values within A, B, C between high and low group were different ($P \leq 0.05$) and indicated with a star.

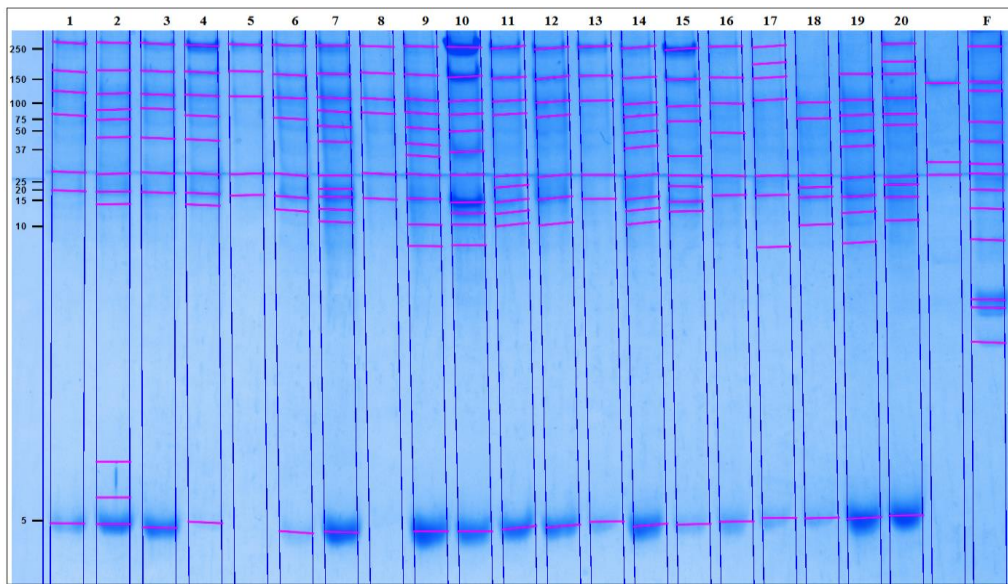


Figure 3.5 Coomassie Blue staining of the Acidic-Acid-Urea (AAU) gel

Results of the AAU gel system where sperm nuclear proteins from different bulls (low fertility bulls: 1-10 and high fertility bulls: 11-20, F: fibroblasts) stained using Coomassie Blue staining, followed by detection of the molecular weights of Protamine1 (PRM1) (5kDa) and histones (around 14-17kDa).

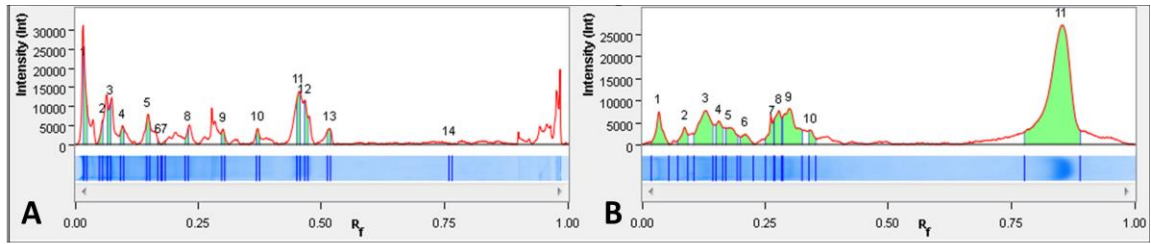


Figure 3.6 Band Intensities of Coomassie Blue staining

Following Coomassie Blue staining, the intensities of two bands from bovine fibroblast cells (negative control) and spermatozoa in the Acidic-Acid-Urea (AAU) gel were evaluated using Image Lab software (Bio-Rad) and represented in figure A and B, respectively. While the x-axis defines the weight of the protein bands, the y-axis represents the intensities of those bands.

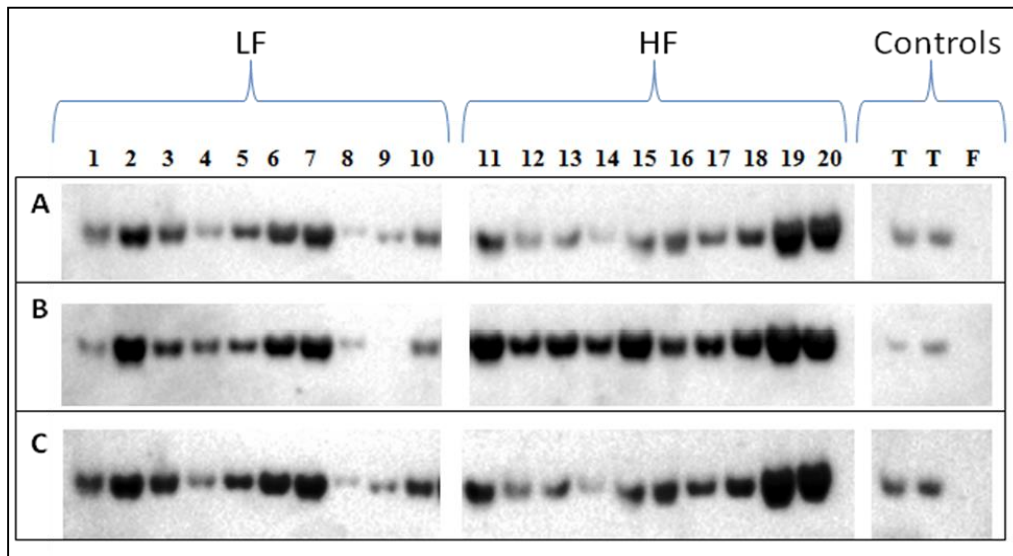


Figure 3.7 Immunoblotting of PRM1

Following immunoblotting, Protamine 1 (PRM1) profiling of sperm from 20 bulls with varying fertility was showed in this figure. Low fertility (LF) bulls were from Line 1 to 10 and high fertility bulls (HF) were from Line 11 to 20 in the figure. While bovine fibroblasts (F) were used as a negative control, bull testis lysate (T) was used as a positive control. Three replicates of western blotting experiments are displayed in A, B and C, respectively.

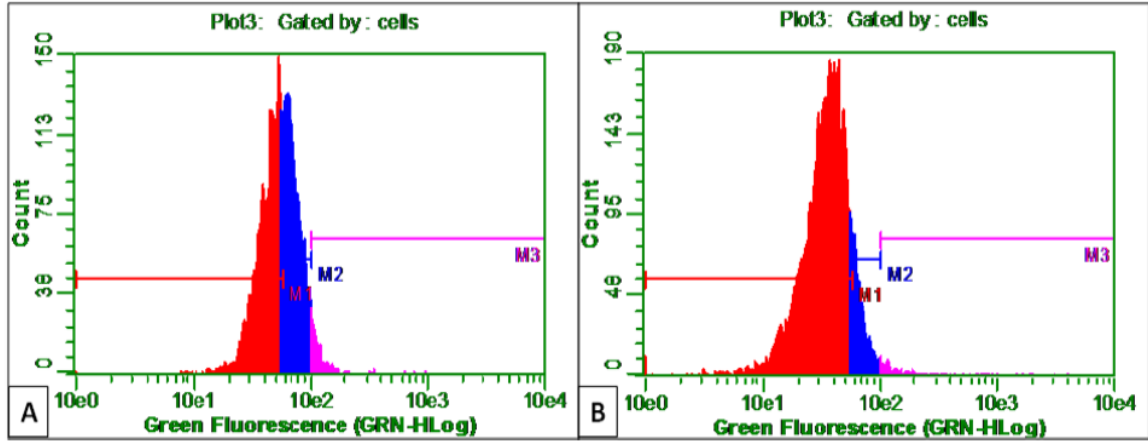


Figure 3.8 Flow Cytometric histograms

Flow cytometric measurements of Protamine1 (PRM1) in spermatozoa from high fertility bulls (A and B, respectively) are displayed as a histogram using three fluorescence markers containing M1, M2 and M3 plots. M1: The area representing a limited/absent fluorescence peak of PRM1, M2: The second peak indicating a normal fluorescence intensity of PRM1 and M3: the last peak containing abnormal fluorescence intensity of PRM1.

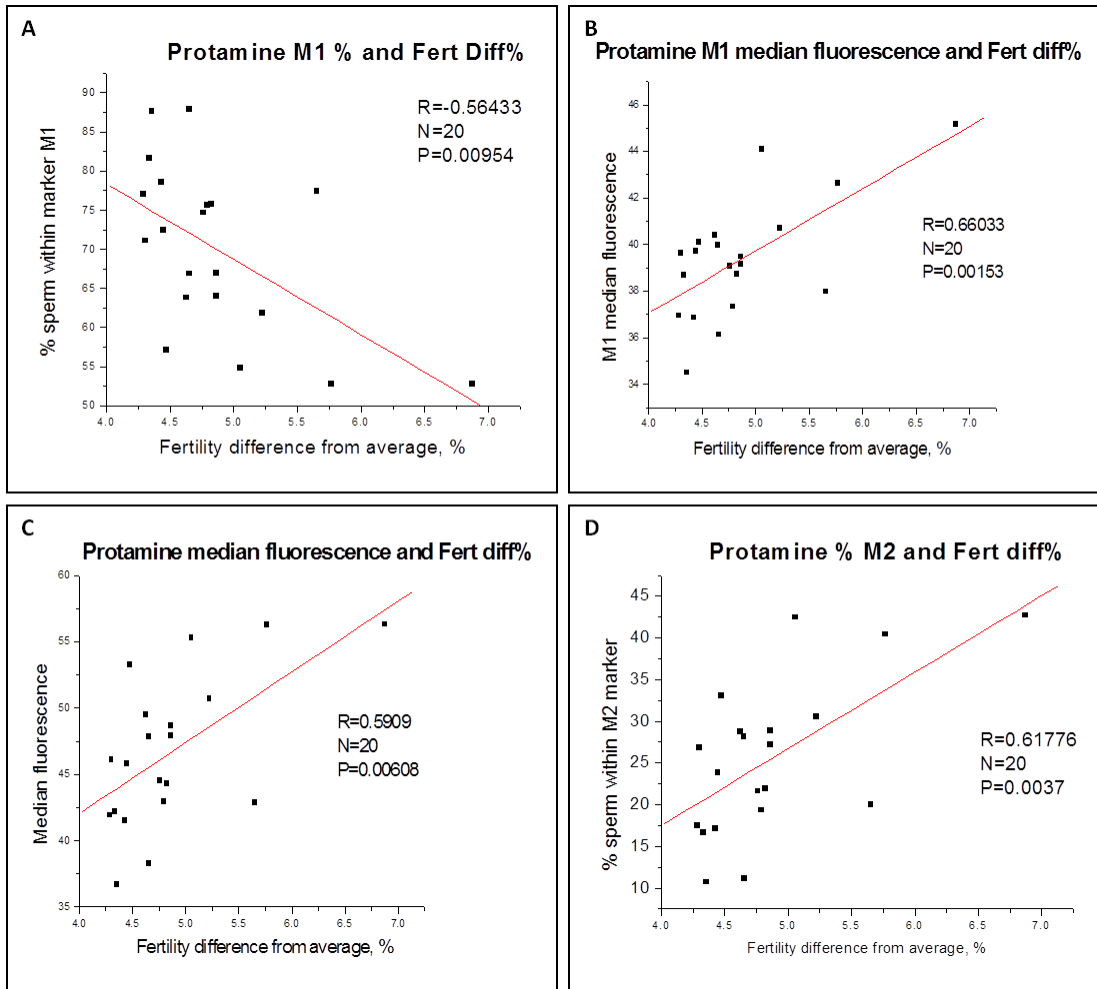


Figure 3.9 Flow Cytometric Plots

According to the flow cytometric results, A) A correlation plot of the percentage of M1 and *in vivo* fertility scores of the bulls is displayed. B) A correlation plot between the Protamine M1 median fluorescence and fertility scores. C) A correlation plot of the median of protamine total fluorescence and 20 bulls with higher fertility. D) The relationship between the rate of M2 and *in vivo* fertility scores of the bulls.

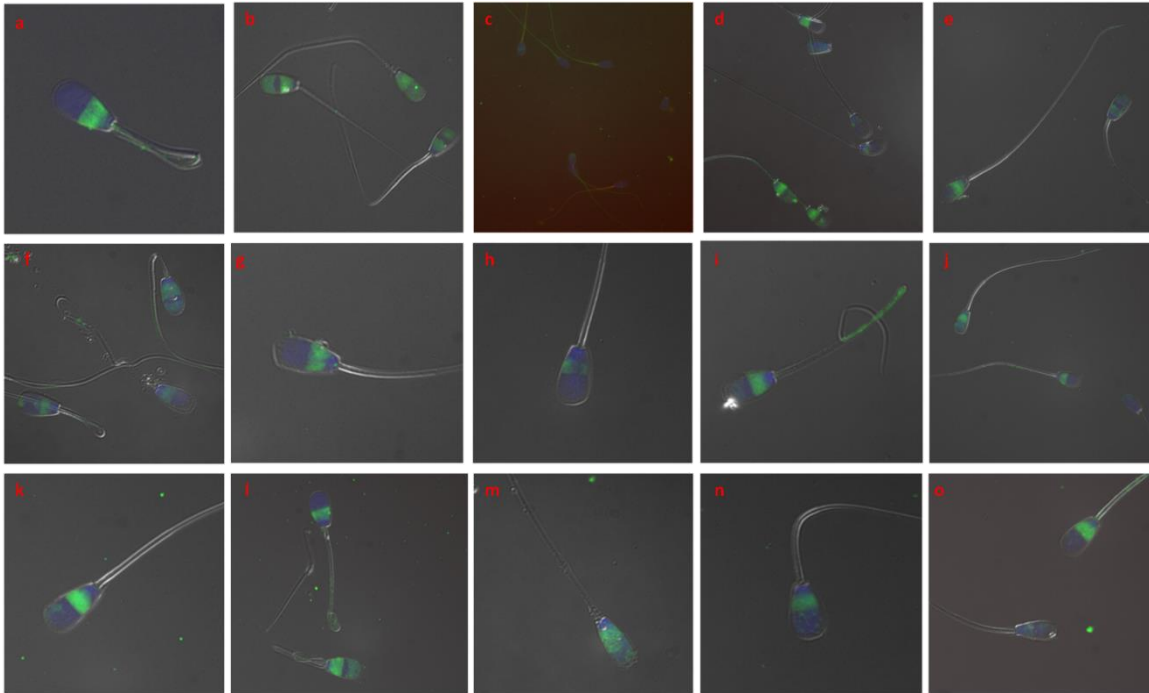


Figure 3.10 Immunocytochemistry Results

Cellular localization of Protamine 1 (PRM1) by ICC. PRM1 localizes in the equatorial and post-equatorial regions of nucleus in sperm with normal morphology (Figure 3.10a), but a scattered localization PRM1 in the pre-equatorial and acrosomal regions abnormal sperm (Figure 3.10d-o). Positive and negative labeling of ICC was also represented in Figure 10b and 10c, respectively. PRM1 (Green), DAPI (blue).

CHAPTER IV

CONCLUSIONS

DNA damage-induced by apoptosis may not be an indicator for male infertility

Germ cell apoptosis during spermatogenesis is essential in the production of sperm [49, 52]. The relationship between DNA damage induced by apoptosis and male infertility is still controversial [1, 2], [3, 4, 58, 59], [60] [43], [61], [62], [63]. Additionally, conventional semen analysis does not include the analysis of sperm DNA and is insufficient to predict reproductive outcomes. Thus, there is a need to develop markers for quantification of male fertility. Sperm DNA damage and apoptosis are either directly or indirectly associated with male infertility; however, details of mechanisms causing DNA damage as well as specific effects of damaged DNA on fertility in the field are not well established. Therefore, the purpose of our specific objective was to investigate the interrelation between male fertility and apoptosis by determining the extent of DNA damage and expression of pro- and anti-apoptotic proteins; BAX and BCL-2, respectively.

According to our results of this specific objective, we demonstrated that DNA damage induced by apoptosis and PS translocation were not correlated to male fertility. The expression of the pro-apoptotic protein BAX in sperm from low fertility bulls was similar and the expression of Bcl-2 was not detectable in spermatozoa of any bulls in this study. We concluded that pro- and anti- apoptotic proteins might be expressed with a

balance in spermatozoa. The most relevant fertility markers might be the percentage of necrotic spermatozoa detected by flow cytometry and live spermatozoa determined via eosin-nigrosin staining. Since we did not find any correlation between DNA fragmentation and PS translocation, we speculated that DNA damage in spermatozoa might have been originated from another cause such as oxidative stress. Because oxidative stress is also associated with apoptosis, they may affect each other in many ways. Oxidative stress may directly induce DNA fragmentation or trigger apoptosis [5]. We did not focus on the activities of caspases. Therefore, our research should be extended to evaluate oxidative DNA damage and caspase activities for further analysis. According to our results, apoptotic markers may not be reliable to predict male infertility in bulls. Since we performed our study using cryopreserved spermatozoa, we should consider the cryo-damage during freezing and thawing processes. Hence, we suggest that apoptosis might be induced during spermatogenesis and spermatozoa rapidly undergo necrosis following cryopreservation. Therefore, necrosis might be the primary pathway that influences sperm viability after thawing. Thus, further clinical studies should be performed to determine the molecular mechanism of the intrinsic apoptotic pathways including the expression and roles of caspases.

Proper condensation of chromatin in sperm is important for sperm function

In mature spermatozoa, histone-packaged chromatin is more susceptible to DNA damage than the protamine-packaged DNA [64]. Protamines are important during chromatin condensation, and abnormal chromatin packaging can affect the accuracy of the paternal gene transition following fertilization [126]. Sperm chromatin packaging anomalies were demonstrated to be related to sub-par fertility in humans [29, 64].

Damages to sperm chromatin negatively affect assisted and natural fertility; thus, sperm DNA should be considered in semen evaluation [127]. Since apoptosis was not the origin of DNA damage in spermatozoa from bulls in our experimental groups, the alterations of sperm chromatin packaging during spermatogenesis might have been the cause of DNA damage in bull spermatozoa. Therefore, our specific objective was to determine the expression dynamics of PRM1 and chromatin structure in sperm from bulls with distinct fertility scores.

Sperm protamination were detectable using toluidine blue in bulls and the proper protamination was significantly decreased in low fertility bulls compared to their highly fertile counterparts. Our findings supported the results of a previous study [114], and we also found that the Halomax test based on the sperm chromatin dispersion method could determine spermatozoa with fragmented DNA via light microscopy. Additionally, sperm chromatin condensation was found to be one of two parameters to estimate bull fertility in our study. We supported the previous report that the assessment of sperm DNA fragmentation (SDF) by Halomax might be a predictor for a successful artificial insemination (AI) in the field [119]. As previously published, mature bull spermatozoa only express PRM1 [27, 28], and our study displayed that the Protamine 1 protein (PRM1) was abundant in spermatozoa from high fertility bulls and was positively related to male fertility. According to our immunocytochemistry results, unlike normal spermatozoa, abnormal spermatozoa showed a scattered localization of PRM1 in the pre-equatorial and acrosomal regions of their nuclei. We concluded that the cause of improper chromatin packaging during spermatogenesis might be the limited expression and/or mislocalization of PRM1. Although we found the difference in the expression

pattern of PRM1 by immunoblotting, this was not found to be an estimator for fertility score in bulls according to our multiple regression analysis. We concluded that sperm defective chromatin condensation and protamination errors were significantly reduced in sperm from high fertility bulls. Therefore, we suggest that evaluating sperm chromatin integrity by detecting protamination status and fragmentation pattern might be sufficient to predict bull fertility in the field. The current study is the first study identifying the dynamics of PRM1 landscape in spermatozoa from bulls with distinct fertility phenotypes. In this study, we speculate that this unique expression of PRM1 in bovine mature spermatozoa might be used as a model in studies where sperm chromatin condensation in mammals is concerned.

REFERENCES

1. Sakkas, D., et al., Origin of DNA damage in ejaculated human spermatozoa. *Rev Reprod*, 1999. **4**(1): p. 31-7.
2. Henkel, R., et al., Influence of deoxyribonucleic acid damage on fertilization and pregnancy. *Fertil Steril*, 2004. **81**(4): p. 965-72.
3. Simon, L., et al., Sperm DNA damage measured by the alkaline Comet assay as an independent predictor of male infertility and in vitro fertilization success. *Fertil Steril*, 2011. **95**(2): p. 652-7.
4. Aitken, R.J., et al., Apoptosis in the germ line. *Reproduction*, 2011. **141**(2): p. 139-50.
5. Agarwal, A., K. Makker, and R. Sharma, Clinical relevance of oxidative stress in male factor infertility: an update. *Am J Reprod Immunol*, 2008. **59**(1): p. 2-11.
6. Sadler, T.W. and J. Langman, *Langman's Essential Medical Embryology*. 2005: Lippincott Williams & Wilkins.
7. Dejarnette, J.M., The effect of semen quality on reproductive efficiency. *Vet Clin North Am Food Anim Pract*, 2005. **21**(2): p. 409-18.
8. Rodriguez-Osorio, N., S. Dogan, and E. Memili, Epigenetics of Mammalian Gamete and Embryo Development, in *Livestock Epigenetics Vol. 1*. 2012: Wiley-Blackwell, Oxford, UK.
9. Govindaraju, A., et al., Delivering value from sperm proteomics for fertility. *Cell Tissue Res*, 2012. **349**(3): p. 783-93.
10. Mays-Hoopers, L.L., et al., Preparation of spermatogonia, spermatocytes, and round spermatids for analysis of gene expression using fluorescence-activated cell sorting. *Biol Reprod*, 1995. **53**(5): p. 1003-11.
11. Lie, P.P., C.Y. Cheng, and D.D. Mruk, Coordinating cellular events during spermatogenesis: a biochemical model. *Trends Biochem Sci*, 2009. **34**(7): p. 366-73.

12. Phillips, B.T., K. Gassei, and K.E. Orwig, Spermatogonial stem cell regulation and spermatogenesis. *Philos Trans R Soc Lond B Biol Sci*, 2010. **365**(1546): p. 1663-78.
13. Aitken, R.J., G.N. De Iuliis, and R.I. McLachlan, Biological and clinical significance of DNA damage in the male germ line. *Int J Androl*, 2009. **32**(1): p. 46-56.
14. Ashwood-Smith, M.J. and R.G. Edwards, DNA repair by oocytes. *Mol Hum Reprod*, 1996. **2**(1): p. 46-51.
15. Seli, E. and D. Sakkas, Spermatozoal nuclear determinants of reproductive outcome: implications for ART. *Hum Reprod Update*, 2005. **11**(4): p. 337-49.
16. Agarwal, A., R.A. Saleh, and M.A. Bedaiwy, Role of reactive oxygen species in the pathophysiology of human reproduction. *Fertil Steril*, 2003. **79**(4): p. 829-43.
17. Miller, D., M. Brinkworth, and D. Iles, Paternal DNA packaging in spermatozoa: more than the sum of its parts? DNA, histones, protamines and epigenetics. *Reproduction*, 2010. **139**(2): p. 287-301.
18. Ward, W.S. and D.S. Coffey, DNA packaging and organization in mammalian spermatozoa: comparison with somatic cells. *Biol Reprod*, 1991. **44**(4): p. 569-74.
19. Ward, W.S., Deoxyribonucleic acid loop domain tertiary structure in mammalian spermatozoa. *Biol Reprod*, 1993. **48**(6): p. 1193-201.
20. Shaman, J.A., Y. Yamauchi, and W.S. Ward, Function of the sperm nuclear matrix. *Arch Androl*, 2007. **53**(3): p. 135-40.
21. Gill-Sharma, M.K., J. Choudhuri, and S. D'Souza, Sperm chromatin protamination: an endocrine perspective. *Protein Pept Lett*, 2011. **18**(8): p. 786-801.
22. Albig, W., et al., The human replacement histone H3.3B gene (H3F3B). *Genomics*, 1995. **30**(2): p. 264-72.
23. Govin, J., et al., The role of histones in chromatin remodelling during mammalian spermiogenesis. *Eur J Biochem*, 2004. **271**(17): p. 3459-69.
24. Tovich, P.R. and R.J. Oko, Somatic Histones Are Components of the Perinuclear Theca in Bovine Spermatozoa. *J. Biol. Chem.* , 2003. **278**: p. 32431–32438.
25. Balhorn, R., S. Reed, and N. Tanphaichitr, Aberrant protamine 1/protamine 2 ratios in sperm of infertile human males. *Experientia*, 1988. **44**(1): p. 52-5.

26. Cho, C., et al., Protamine 2 deficiency leads to sperm DNA damage and embryo death in mice. *Biol Reprod*, 2003. **69**(1): p. 211-7.
27. Dobrinski, I., H.P. Hughes, and A.D. Barth, Flow cytometric and microscopic evaluation and effect on fertility of abnormal chromatin condensation in bovine sperm nuclei. *J Reprod Fertil*, 1994. **101**(3): p. 531-8.
28. Yamauchi, Y., J.A. Shaman, and W.S. Ward, Non-genetic contributions of the sperm nucleus to embryonic development. *Asian J Androl*, 2011. **13**(1): p. 31-5.
29. Oliva, R., Protamines and male infertility. *Hum Reprod Update*, 2006. **12**(4): p. 417-35.
30. Vilfan, I.D., C.C. Conwell, and N.V. Hud, Formation of native-like mammalian sperm cell chromatin with folded bull protamine. *J Biol Chem*, 2004. **279**(19): p. 20088-95.
31. Brewer, L., et al., Dynamics of protamine 1 binding to single DNA molecules. *J Biol Chem*, 2003. **278**(43): p. 42403-8.
32. Kerr, J.F., History of the events leading to the formulation of the apoptosis concept. *Toxicology*, 2002. **181-182**: p. 471-4.
33. Elmore, S., Apoptosis: a review of programmed cell death. *Toxicol Pathol*, 2007. **35**(4): p. 495-516.
34. Lachaud, C., et al., Apoptosis and necrosis in human ejaculated spermatozoa. *Hum Reprod*, 2004. **19**(3): p. 607-10.
35. Sharma, R.K., T. Said, and A. Agarwal, Sperm DNA damage and its clinical relevance in assessing reproductive outcome. *Asian J Androl*, 2004. **6**(2): p. 139-48.
36. Singh, N.P., C.H. Muller, and R.E. Berger, Effects of age on DNA double-strand breaks and apoptosis in human sperm. *Fertil Steril*, 2003. **80**(6): p. 1420-30.
37. Sepaniak, S., et al., The influence of cigarette smoking on human sperm quality and DNA fragmentation. *Toxicology*, 2006. **223**(1-2): p. 54-60.
38. Shekarriz, M., et al., A method of human semen centrifugation to minimize the iatrogenic sperm injuries caused by reactive oxygen species. *Eur Urol*, 1995. **28**(1): p. 31-5.
39. Mortimer, D., Sperm preparation methods. *J Androl*, 2000. **21**(3): p. 357-66.

40. Cocuzza, M., et al., Clinical relevance of oxidative stress and sperm chromatin damage in male infertility: an evidence based analysis. *Int Braz J Urol*, 2007. **33**(5): p. 603-21.
41. Fernandez, J.L., et al., Halosperm is an easy, available, and cost-effective alternative for determining sperm DNA fragmentation. *Fertil Steril*, 2005. **84**(4): p. 860.
42. Garcia-Macias, V., et al., DNA fragmentation assessment by flow cytometry and Sperm-Bos-Halomax (bright-field microscopy and fluorescence microscopy) in bull sperm. *Int J Androl*, 2007. **30**(2): p. 88-98.
43. Morris, I.D., et al., The spectrum of DNA damage in human sperm assessed by single cell gel electrophoresis (Comet assay) and its relationship to fertilization and embryo development. *Hum Reprod*, 2002. **17**(4): p. 990-8.
44. Agarwal, A. and T.M. Said, Role of sperm chromatin abnormalities and DNA damage in male infertility. *Hum Reprod Update*, 2003. **9**: p. 331-34.
45. Sikka, S.C., Role of oxidative stress and antioxidants in andrology and assisted reproductive technology. *J Androl*, 2004. **25**(1): p. 5-18.
46. Zini, A. and J. Libman, Sperm DNA damage: clinical significance in the era of assisted reproduction. *CMAJ*, 2006. **175**(5): p. 495-500.
47. Blaschek, M., et al., A whole-genome association analysis of noncompensatory fertility in Holstein bulls. *J Dairy Sci*, 2011. **94**(9): p. 4695-9.
48. Sakkas, D., et al., Nature of DNA damage in ejaculated human spermatozoa and the possible involvement of apoptosis. *Biol Reprod*, 2002. **66**(4): p. 1061-7.
49. Marchetti, C., et al., Study of mitochondrial membrane potential, reactive oxygen species, DNA fragmentation and cell viability by flow cytometry in human sperm. *Hum Reprod*, 2002. **17**(5): p. 1257-65.
50. Paasch, U., et al., Activation pattern of caspases in human spermatozoa. *Fertil Steril*, 2004. **81 Suppl 1**: p. 802-9.
51. Ricci, G., et al., Semen preparation methods and sperm apoptosis: swim-up versus gradient-density centrifugation technique. *Fertil Steril*, 2009. **91**(2): p. 632-8.
52. Anzar, M., et al., Sperm apoptosis in fresh and cryopreserved bull semen detected by flow cytometry and its relationship with fertility. *Biol Reprod*, 2002. **66**(2): p. 354-60.
53. Martin, G., et al., Cryopreservation induces an apoptosis-like mechanism in bull sperm. *Biol Reprod*, 2004. **71**(1): p. 28-37.

54. Martin, G., et al., Kinetics of occurrence of some features of apoptosis during the cryopreservation process of bovine spermatozoa. *Hum Reprod*, 2007. **22**(2): p. 380-8.
55. Chaveiro, A., P. Santos, and F.M. da Silva, Assessment of sperm apoptosis in cryopreserved bull semen after swim-up treatment: a flow cytometric study. *Reprod Domest Anim*, 2007. **42**(1): p. 17-21.
56. Gong, Y., et al., Nonylphenol induces apoptosis in rat testicular Sertoli cells via endoplasmic reticulum stress. *Toxicol Lett*, 2009. **186**(2): p. 84-95.
57. Chen, W.S., et al., Growth retardation and increased apoptosis in mice with homozygous disruption of the Akt1 gene. *Genes Dev*, 2001. **15**(17): p. 2203-8.
58. Waterhouse, K.E., et al., Sperm DNA damage is related to field fertility of semen from young Norwegian Red bulls. *Reprod Fertil Dev*, 2006. **18**(7): p. 781-8.
59. Colombero, L.T., et al., Incidence of sperm aneuploidy in relation to semen characteristics and assisted reproductive outcome. *Fertil Steril*, 1999. **72**(1): p. 90-6.
60. Weng, S.L., et al., Caspase activity and apoptotic markers in ejaculated human sperm. *Mol Hum Reprod*, 2002. **8**(11): p. 984-91.
61. Henkel, R., et al., DNA fragmentation of spermatozoa and assisted reproduction technology. *Reprod Biomed Online*, 2003. **7**(4): p. 477-84.
62. Khalili, M.A., et al., Sperm nuclear DNA in ejaculates of fertile and infertile men: correlation with semen parameters. *Urol J*, 2006. **3**(3): p. 154-9.
63. Bakos, H.W., et al., Sperm DNA damage is associated with assisted reproductive technology pregnancy. *Int J Androl*, 2008. **31**(5): p. 518-26.
64. Aoki, V.W., et al., Sperm protamine 1/protamine 2 ratios are related to in vitro fertilization pregnancy rates and predictive of fertilization ability. *Fertil Steril*, 2006. **86**(5): p. 1408-15.
65. de Mateo, S., et al., Protamine 2 precursors (Pre-P2), protamine 1 to protamine 2 ratio (P1/P2), and assisted reproduction outcome. *Fertil Steril*, 2009. **91**(3): p. 715-22.
66. Zini, A., S.M. Gabriel, and X. Zhang, The histone to protamine ratio in human spermatozoa: comparative study of whole and processed semen. *87*, 2006. **1**: p. 217-219.
67. Setchell, B.P., et al., Is embryonic mortality increased in normal female rats mated to subfertile males? *J Reprod Fertil*, 1988. **82**(2): p. 567-74.

68. Spano, M., et al., Sperm chromatin damage impairs human fertility. The Danish First Pregnancy Planner Study Team. *Fertil Steril*, 2000. **73**(1): p. 43-50.
69. Vaux, D.L. and S.J. Korsmeyer, Cell death in development. *Cell*, 1999. **96**(2): p. 245-54.
70. Reed, J.C., Proapoptotic multidomain Bcl-2/Bax-family proteins: mechanisms, physiological roles, and therapeutic opportunities. *Cell Death Differ*, 2006. **13**(8): p. 1378-86.
71. Pena, F.J., et al., Mitochondria in mammalian sperm physiology and pathology: a review. *Reprod Domest Anim*, 2009. **44**(2): p. 345-9.
72. Peddinti, D., et al., Comprehensive proteomic analysis of bovine spermatozoa of varying fertility rates and identification of biomarkers associated with fertility. *BMC Systems Biology* 2008. **2**(19).
73. Zwald, N.R., et al., Genetic selection for health traits using producer-recorded data. II. Genetic correlations, disease probabilities, and relationships with existing traits. *J Dairy Sci*, 2004. **87**(12): p. 4295-302.
74. Zwald, N.R., et al., Genetic selection for health traits using producer-recorded data. I. Incidence rates, heritability estimates, and sire breeding values. *J Dairy Sci*, 2004. **87**(12): p. 4287-94.
75. Chang, Y.M., et al., Effects of trait definition on genetic parameter estimates and sire evaluation for clinical mastitis with threshold models. *Animal Science*, 2004. **79**: p. 355-363.
76. D'Amours, O., et al., Proteomic comparison of detergent-extracted sperm proteins from bulls with different fertility indexes. *Reproduction*, 2010. **139**(3): p. 545-56.
77. Absalan, F., et al., Value of sperm chromatin dispersion test in couples with unexplained recurrent abortion. *J Assist Reprod Genet*, 2012. **29**(1): p. 11-4.
78. Felipe-Perez, Y.E., et al., Viability of fresh and frozen bull sperm compared by two staining techniques. *Acta Veterinaria Brasilica* 2008. **2**: p. 123-130.
79. Dott, H.M. and G.C. Foster, A technique for studying the morphology of mammalian spermatozoa which are eosinophilic in a differential 'life-dead' stain. *J Reprod Fertil*, 1972. **29**(3): p. 443-5.
80. Laemmli, U.K., Cleavage of structural proteins during the assembly of the head of bacteriophage T4. *Nature*, 1970. **227**(5259): p. 680-5.
81. Oltvai, Z.N. and S.J. Korsmeyer, Checkpoints of dueling dimers foil death wishes. *Cell*, 1994. **79**(2): p. 189-92.

82. Knudson, C.M., et al., Bax-deficient mice with lymphoid hyperplasia and male germ cell death. *Science*, 1995. **270**(5233): p. 96-9.
83. Zhang, Z.H., et al., Expression of Bcl-2 and Bax in rhesus monkey testis during germ cell apoptosis induced by testosterone undecanoate. *Arch Androl*, 2003. **49**(6): p. 439-47.
84. Woolveridge, I., et al., Apoptosis and expression of apoptotic regulators in the human testis following short- and long-term anti-androgen treatment. *Mol Hum Reprod*, 1998. **4**(7): p. 701-7.
85. Hendricks, K.E. and P.J. Hansen, Can programmed cell death be induced in post-ejaculatory bull and stallion spermatozoa? *Theriogenology*, 2009. **71**(7): p. 1138-46.
86. Benchaib, M., et al., Sperm DNA fragmentation decreases the pregnancy rate in an assisted reproductive technique. *Hum Reprod*, 2003. **18**(5): p. 1023-8.
87. Zhuang, Z., et al., Mutations of the MEN1 tumor suppressor gene in pituitary tumors. *Cancer Res*, 1997. **57**(24): p. 5446-51.
88. Brahem, S., et al., Semen processing by density gradient centrifugation is useful in selecting sperm with higher double-strand DNA integrity. *Andrologia*, 2011. **43**(3): p. 196-202.
89. Khan, D.R., et al., Apoptosis in fresh and cryopreserved buffalo sperm. *Theriogenology*, 2009. **71**(5): p. 872-6.
90. Nur, Z., et al., Effects of different cryoprotective agents on ram sperm morphology and DNA integrity. *Theriogenology*, 2010. **73**(9): p. 1267-75.
91. Said, T.M., A. Gaglani, and A. Agarwal, Implication of apoptosis in sperm cryoinjury. *Reprod Biomed Online*, 2010. **21**(4): p. 456-62.
92. Ward, W.S., Function of sperm chromatin structural elements in fertilization and development. *Mol Hum Reprod*, 2010. **16**(1): p. 30-6.
93. Balhorn, R., The protamine family of sperm nuclear proteins. *Genome Biol*, 2007. **8**(9): p. 227.
94. Talbert, P.B. and S. Henikoff, Histone variants--ancient wrap artists of the epigenome. *Nat Rev Mol Cell Biol*, 2010. **11**(4): p. 264-75.
95. Brykczynska, U., et al., Repressive and active histone methylation mark distinct promoters in human and mouse spermatozoa. *Nat Struct Mol Biol*, 2010. **17**(6): p. 679-87.

96. Gardiner-Garden, M., et al., Histone- and protamine-DNA association: conservation of different patterns within the beta-globin domain in human sperm. *Mol Cell Biol*, 1998. **18**(6): p. 3350-6.
97. Gill, M.E., S. Erkek, and A.H. Peters, Parental epigenetic control of embryogenesis: a balance between inheritance and reprogramming? *Curr Opin Cell Biol*, 2012. **24**(3): p. 387-96.
98. Marushige, Y. and K. Marushige, Dispersion of mammalian sperm chromatin during fertilization: an in vitro study. *Biochim Biophys Acta*, 1978. **519**(1): p. 1-22.
99. Karoui, S., et al., Is sperm DNA fragmentation a good marker for field AI bull fertility? *J Anim Sci*, 2012. **90**(8): p. 2437-49.
100. Gosalvez, J., et al., Relationships between the dynamics of iatrogenic DNA damage and genomic design in mammalian spermatozoa from eleven species. *Mol Reprod Dev*, 2011. **78**(12): p. 951-61.
101. Fortes, M.R., et al., The integrity of sperm chromatin in young tropical composite bulls. *Theriogenology*, 2012. **78**(2): p. 326-33, 333 e1-4.
102. Urbano, M., et al., 84 effect of a stressor on canine sperm DNA fragmentation using the sperm chromatin dispersion test. *Reprod Fertil Dev*, 2012. **25**(1): p. 189-90.
103. Lopez-Fernandez, C., et al., Fragmentation dynamics of frozen-thawed ram sperm DNA is modulated by sperm concentration. *Theriogenology*, 2010. **74**(8): p. 1362-70.
104. Parrilla, I., et al., Differences in the ability of spermatozoa from individual boar ejaculates to withstand different semen-processing techniques. *Anim Reprod Sci*, 2012. **132**(1-2): p. 66-73.
105. Gonzalez-Marin, C., et al., Bacteria in bovine semen can increase sperm DNA fragmentation rates: a kinetic experimental approach. *Anim Reprod Sci*, 2011. **123**(3-4): p. 139-48.
106. Fernandez, J.L., et al., Simple determination of human sperm DNA fragmentation with an improved sperm chromatin dispersion test. *Fertil Steril*, 2005. **84**(4): p. 833-42.
107. Evenson, D.P. and R. Wixon, Comparison of the Halosperm test kit with the sperm chromatin structure assay (SCSA) infertility test in relation to patient diagnosis and prognosis. *Fertil Steril*, 2005. **84**(4): p. 846-9.

108. Enciso, M., et al., Infertile men with varicocele show a high relative proportion of sperm cells with intense nuclear damage level, evidenced by the sperm chromatin dispersion test. *J Androl*, 2006. **27**(1): p. 106-11.
109. Hecht, N., et al., Protamine-1 represents a sperm specific gene transcript: a study in *Callithrix jacchus* and *Bos taurus*. *Andrologia*, 2011. **43**(3): p. 167-73.
110. Cho, C., et al., Haploinsufficiency of protamine-1 or -2 causes infertility in mice. *Nat Genet*, 2001. **28**(1): p. 82-6.
111. Martins, R.P. and S.A. Krawetz, Decondensing the protamine domain for transcription. *Proc Natl Acad Sci U S A*, 2007. **104**(20): p. 8340-5.
112. Marushige, Y. and K. Marushige, Transformation of sperm histone during formation and maturation of rat spermatozoa. *J Biol Chem*, 1975. **250**(1): p. 39-45.
113. Pirhonen, A., A. Linnala-Kankkunen, and P.H. Maenpaa, Identification of phosphoserine residues in protamines from mature mammalian spermatozoa. *Biol Reprod*, 1994. **50**(5): p. 981-6.
114. Beletti, M.E. and M.L. Mello, Comparison between the toluidine blue stain and the Feulgen reaction for evaluation of rabbit sperm chromatin condensation and their relationship with sperm morphology. *Theriogenology*, 2004. **62**(3-4): p. 398-402.
115. de Yebra, L. and R. Oliva, Rapid analysis of mammalian sperm nuclear proteins. *Anal Biochem*, 1993. **209**(1): p. 201-3.
116. Odhiambo, J.F., et al., Adaptation of ubiquitin-PNA based sperm quality assay for semen evaluation by a conventional flow cytometer and a dedicated platform for flow cytometric semen analysis. *Theriogenology*, 2011. **76**(6): p. 1168-76.
117. Sutovsky, P., Visualization of sperm accessory structures in the mammalian spermatids, spermatozoa, and zygotes by immunofluorescence, confocal, and immunoelectron microscopy. *Methods Mol Biol*, 2004. **253**: p. 59-77.
118. Sutovsky, P., R. Hauser, and M. Sutovsky, Increased levels of sperm ubiquitin correlate with semen quality in men from an andrology laboratory clinic population. *Hum Reprod*, 2004. **19**(3): p. 628-38.
119. Karoui, S., et al., Is sperm DNA fragmentation a good marker for field AI bull fertility. *Journal of animal science*, 2012.
120. Feugang, J.M., et al., Transcriptome analysis of bull spermatozoa: implications for male fertility. *Reprod Biomed Online*, 2010. **21**(3): p. 312-24.

121. Jenkins, T.G. and D.T. Carrell, The paternal epigenome and embryogenesis: poisoning mechanisms for development. *Asian J Androl*, 2011. **13**(1): p. 76-80.
122. de Yebra, L., et al., Detection of P2 precursors in the sperm cells of infertile patients who have reduced protamine P2 levels. *Fertil Steril*, 1998. **69**(4): p. 755-9.
123. Mengual, L., et al., Marked differences in protamine content and P1/P2 ratios in sperm cells from percoll fractions between patients and controls. *J Androl*, 2003. **24**(3): p. 438-47.
124. Hammadeh, M.E., et al., Protamine contents and P1/P2 ratio in human spermatozoa from smokers and non-smokers. *Hum Reprod*, 2010. **25**(11): p. 2708-20.
125. Depa-Martynow, M., et al., Impact of protamine transcripts and their proteins on the quality and fertilization ability of sperm and the development of preimplantation embryos. *Reprod Biol*, 2012. **12**(1): p. 57-72.
126. Tesarik, J., E. Greco, and C. Mendoza, Late, but not early, paternal effect on human embryo development is related to sperm DNA fragmentation. *Hum Reprod*, 2004. **19**(3): p. 611-5.
127. Aziz, N., et al., The relationship between human sperm apoptosis, morphology and the sperm deformity index. *Hum Reprod*, 2007. **22**(5): p. 1413-19

APPENDIX A
SUPPLEMENTARY PROTOCOLS

Fibroblast Cell Culture Protocol

Primary Fibroblast Culture

- | | |
|--|------|
| 1) Basal medium Eagle (BME) | 80ml |
| 2) Foetal bovine serum | 20ml |
| 3) Penicillin-streptomycin solution 100x | 1ml |

**Filter and store at +4°C (up to 1 month) **

The skin biopsy sample should be shaped as a diamond and about 5-10 mm in diameter (collect the tissue sample in sterile BME fibroblast medium)

Procedure 1

- 1) Rapidly wash the skin biopsy in PBS in a Petri dish, cut into small fragments and transfer these to a flask.
- 2) Using a sterile Pasteur pipette with flame-rounded tip, distribute the small tissue fragments over the bottom surface of the culture flask.
- 3) Pass the flask rapidly and carefully through the Bunsen flame in order to evaporate the medium so that the minced tissue pieces adhere to the plastic surface, but so as not to heat-damage the minced tissue. Take care not to cook the tissue!
- 4) Carefully add BME medium for fibroblast growth, firmly close the lid of the flask and place in CO₂ incubator.
- 5) The next day, slightly unscrew the lid of the flask so that the tissue can “breathe.”

- 6) Replace the culture medium after two days and, from this point on, replace it three times a week.
- 7) The fibroblasts will start to grow from the minced fragments in 2-3 days. When there are sufficient cells, they are detached enzymatically and plated in Petri dishes, or 75 cm² culture flasks, for proliferation (see next steps: “Maintenance of cell cultures in dishes and flasks” and “Routine subculture of adherent cell lines”). The minced fragments in the flask will continue to produce cells for a while.

Regular Maintenance of Cultured Cells

DMEM + Glutamax Cell Culture Media

1) DMEM + Glutamax	44.5ml (cell culture fridge)	22.250ml
2) FBS	5ml (cell culture freezer)	2.5ml
3) Hyclone	500µl (cell culture freezer)	250ul
Total	50ml	25ml

Procedure

- 1) All components, listed above, are mixed in a 50ml Falcon tube, and then filtered by using 25µm filter under laminar flow.
- 2) After media preparation, the tube should be wiped with 70% ethanol and placed in the incubator.

- 3) The general morphology and growth of a cell population, as well as the presence of any microbial contaminants, should be checked regularly under an inverted microscope in phase contrast.
- 4) For dishes with non-confluent cells the medium is discarded and replaced with fresh medium:
 - a. T-25: ~5ml (media should be discarded with glass pipette under proper conditions)
 - b. T-75: ~15-20ml (media should be discarded with glass pipette under proper conditions)
- 5) Dishes or flasks with cells at about 70% confluence are treated with trypsin; the cells are then harvested and either frozen or divided for further proliferation (see below “Cell Culture Expansion and Freezing”).
- 6) Medium has to be every 2-4 days after expansion.

Trypsinization (Expansion) of Cells

Materials

- ✓ Trypsin
- ✓ PBS
- ✓ Culture Media

Procedure 1

- 1) Remove culture media with glass pipette. Remember to sterilize pipette before placement into flask.
- 2) Add trypsin (1.5-2 ml for T-25; 4.5-5ml for T-75) to flask and place in incubator for 3-5 minutes by racking frequently.
- 3) Observe the cells under the microscope: if they are seen to be rounded, they are detached, if most are not rounded, leave the suspension in the incubator for a further minute or two (until rounded).
- 4) Remove trypsin and place in 15ml falcon tube.
- 5) Wash with pre-warmed PBS-FBS by agitating the cells (2.5ml for T-25; 5ml for T-75).
- 6) Remove PBS and place into 15ml falcon tube with trypsin.
- 7) Centrifuge tube for 5 minutes (between speed 2&3).
- 8) Remove supernatant, leaving pellet undisturbed.
- 9) Add 1ml of pre-warmed culture media, resuspend.
- 10) Label new flask with date and passage
- 11) Put fresh media into new flask (5ml for T-25; 15-20ml for T-75).
- 12) Equally distribute suspension into new flask(s).

Procedure 2 (preparation of the fibroblast cells for further use)

- 1) Complete steps 1-8
- 2) Add cold PBS PI, resuspend

- 3) Aliquot mixture in 1 ml increments into a 1.5ml eppendorf tube labelled with the information
- 4) Centrifuge for 5 minutes in refrigerated centrifuge at 4°C and at highest speed (13)
- 5) Remove supernatant as much as possible
- 6) Store tubes at -80°C

Procedure for counting cells

- 1) Transfer 200 µl of the cell suspension into a 1.5 ml microfuge tube.
- 2) Add 300 µl of PBS and 500 µl of 0.4% trypan blue solution to the cell suspension (creating a dilution factor of 5) in the centrifuge tube.
- 3) Mix thoroughly and allow to stand 5 to 15 minutes. Note: If cells are exposed to trypan blue for
- 4) Extended periods of time, viable cells may begin to take up dye as well as non-viable cells, thus, try to do cell counts within one hour after dye solution is added.
- 5) With a cover-slip in place, use a pasteur pipette and transfer a small amount of the trypan blue-cell suspension to a chamber on the hemacytometer.
- 6) This is done by carefully touching the edge of the cover-slip with the pipette tip and allowing the chamber to fill by capillary action. Do not overfill or under fill the chambers. 20µl USING CAPILARY ACTION should be enough. Do not directly pipette into the chamber.

- 7) Count all the cells (non-viable cells stain blue, viable cells will remain opaque) in the 1mm center square and the four corner squares.
- 8) Refer to diagram above. Keep a separate count of viable and non-viable cells. If greater than 25% of cells are non-viable, the culture is not being maintained on the appropriate amount of media; re-incubate culture and adjust the volume of media according to the confluency of the cells and the appearance of the media.
- 9) If there are less than 50 or more than 200 cells per large square, repeat the procedure adjusting to an appropriate dilution factor.
- 10) Repeat the count using the other chamber of the hemacytometer.
- 11) Each square of the hemacytometer (with cover slip in place) represents a total volume of 0.1 mm³ or 10⁻⁴ cm³. Since 1 cm³ is equivalent to 1 ml, the subsequent cell concentration per ml (and the total number of cells) will be determined using the following calculations.
 - ✓ Cells per ml = the average count per square x the dilution factor x 10⁴ (count 10 squares)
 - ✓ Example: If the average counts per square are 45 cells x 5 x 10⁴ = 2,250,000 or 2.25 x 10⁶ cells/ml.
 - ✓ Total cell number = cells per ml x the original volume of fluid from which cell sample was removed.

Example: 2.25 x 10⁶ (cell per ml) x 10 ml (original volume) = 2.25 x 10⁷ total cells

In practise, calculation may be done by using this equation; for one T-25 flask ~4-
5x10⁶ T-75 flask ~12-15x10⁶

Cryopreservation of fibroblast cells

Freezing of Cells

Materials

- ✓ Trypsin (cell culture freezer)
- ✓ PBS (cell culture fridge)
- ✓ Freezing media (cell culture freezer)

Procedure

- 1) Complete steps 1-8 of “Trypsinization of Cells” procedure.
- 2) Place pre-warmed freezing media into 15ml falcon tube (1-5ml).
- 3) Re-suspend cells and put into cryopreservation tube.
- 4) Place cryo tube into ice for 10 minutes (4°C)
- 5) Keep tube at -80°C overnight
- 6) Store in liquid nitrogen tank

Thawing of Cells

Materials

- ✓ Pre-warmed culture media
- ✓ 15 ml falcon tube

Procedure

- 1) Thaw vial of cryopreserved fibroblast cells in 37°C water bath for 10 min, or until the contents are completely liquid
- 2) Take thawed fibroblast cells and put them in a 15ml falcon tube
- 3) Wash vial with 1-2 ml of pre-warmed culture media or PBS-FBS and add it to the 15 ml falcon tube
- 4) Bring contents in falcon tube up to 5-6 ml
- 5) Centrifuge falcon tube for 5 minutes at a speed of 2-3
- 6) Remove supernatant (as much as possible without disturbing the pellet)
- 7) Add fresh media up to 1 ml
- 8) Put falcon tube back into incubator
- 9) Prepare flasks with fresh media
- 10) Divide the cells evenly between newly prepared flasks

Sperm Isolation Protocol

The Percoll Stock Solution Protocol

10x Stock Solution (Used To Prepare 90% Percoll)

1.0 M KCl (used in 10X stock solution)

A. Ingredients:

1. 745 mg (0.745 gm) KCl

2. Type I reagent grade water

B. Preparation:

1. Weigh KCl.
2. Add 10 ml of water.
3. Sterilize by filtration.

0.1 M NaH_2PO_4 (used in 10X stock solution)

A. Ingredients:

1. 0.0138 g (13, 8 mg) NaH_2PO_4
2. Type I reagent grade water

B. Preparation:

1. Weigh NaH_2PO_2
2. Add 10 ml water.
3. Sterilize by filtration.

Procedure:

1. Add prescribed amounts of chemicals [1.545 mL of 1M KCl and 1.460 mL of 0.1M NaH_2PO_4] and ~30 mL of H_2O .
2. Add 2.337 g of NaCl and 1.190 g of HEPES.
3. Adjust pH to 7.3. (Because it is acidic before the adjustment)
4. Q.S (Bring up) to 50 ml with water.
5. Filter sterilize and store in a plastic tube.

6. Store refrigerated for 3 months. DO NOT FREEZE IT!!

600mg/ml CaCl_2 (used in making 90% percoll)

1. 6 grams $\text{CaCl}_2 \cdot 2\text{H}_2\text{O}$
2. Type I reagent grade water

B. Preparation:

1. Weigh $\text{CaCl}_2 \cdot 2\text{H}_2\text{O}$.
2. Add 10 ml H_2O .
3. Filter sterilize.
4. Store frozen.

200 mg/ml MgCl_2 (used in making 90% percoll)

1. 2 grams $\text{MgCl}_2 \cdot 6\text{H}_2\text{O}$
2. Type I reagent grade water

B. Preparation:

1. Weigh $\text{MgCl}_2 \cdot 6\text{H}_2\text{O}$.
2. Add 10 ml water.
3. Filter sterilize.

Table A.1 Table A 90% Percoll Recipe

4. Store	Company	Addition	Location
frozen.Chemical			
Stock Percoll (%100)	P4937 (Sigma)	22.5 ml	4°C of cell culture lab.
DL-lactic acid (60% Syrup)	L7900	92 µl	
*10X stock Solution		5.0ml	Fresh
Sodium bicarbonate (NaHCO ₃)	S6297	52.25 mg (.209 gm)	Chemical cabinet of the cell culture lab
*Calcium chloride CaCl ₂	C7902	12.06 µl	
*Magnesium chloride hex hydrate MgCl ₂ 6H ₂ O (0.1M)	M2393	100.1 µl	
Pen/strep		250 µl	Freezer
Total		25ml	

Procedure:

1. Prepare in the hood
2. Combine ingredients.
3. Filter sterilizes.
4. Prepare every two weeks and store refrigerated.

Preparation of the Percoll Solution

Protocol:

- 1) Prepare %45 Percoll before start:
- 2) 45% percoll: 90% Percoll and PBS (Ratio 1:1)
- 3) 2ml of 45% Percoll in the Falcon tube (15ml)

- 4) Incubate Percoll gradient solution at 37 °C for 5-10 min.

Sperm Isolation/ Separation

Materials: semen straws, beakers, Percoll gradient pre warmed to room temperature, 15ml Falcon tubes, 1.5 ml Eppendorf tubes, Pasteur pipettes, Hemacytometer, adjusted as room temperature and 4°C centrifuges.

Protocol:

1. After prepare the percoll tubes, let them warm (See related protocol)
2. Thaw 1 straw of semen for each bull in warm tap water 37°C for 1 minute
3. Wipe straw with dry Kim wipe then with alcohol sprayed kimwipe
4. Cut straw and empty layer semen on top of the Percoll gradient, avoiding mixing layers.
5. Falcon tube in the centrifuge, spin at 700 x g (\approx 2200 rpm) for 20 minutes at room temp. (the medium speed)
6. Carefully remove the supernatant by pasteur pipet, leave the sperm pellet into bottom of the tube
7. Add PBS (@37°C) into the Falcon tube for washing and mix by gently agitating the tube.
8. Centrifuge at 700 x g (\approx 2200 rpm) for 7 minutes at room temp. (low speed like 4)
9. Carefully remove the supernatant as much as possible
10. Add new PBS (@37°C)bring it to 1ml
11. Counting of the sperm cells

- 12.** Remove 2 μ l of sperm sample of the stock then add 198 μ l of ddH₂O in 1.5 ml Eppendorf tube, vortex gently (Make sure your stock and your counting tubes should be homogenously mixed)
- 13.** Load into the hemocytometer by 10 μ l of mixture.
Count sperms according to hemocytometer protocol
- 14.** Adjust the sample as 1X10⁶/ ml in PBS then centrifuge at 12,000rpm for 5 minutes at 37°C and remove the supernatant as much as possible.
- 15.** Apply the flow cytometry protocol.